PHOTOCHEMISTRY AND CLOUDS OF JUPITER, SATURN AND URANUS

S.K. Atreya
University of Michigan, Ann Arbor, MI 48109, USA

P.N. Romani
University of Michigan, Ann Arbor, MI 48109, USA

Abstract. Photochemistry of ammonia, methane, phosphine, hydrogen sulfide, methylamine, hydrogen cyanide and carbon monoxide in the atmospheres of Jupiter, Saturn and Uranus is discussed. Condensation of ammonia, ammonium hydrosulfide, water, methane, ethane and acetylene below and near the tropopause of these planets is formulated. Whenever necessary, new calculations are included. Candidates for the upper atmospheric hazes, and the reddish-brown chromophore in the clouds of Jupiter and Saturn are discussed.

1 INTRODUCTION

The outer planets exhibit a reducing atmosphere, which for all practical purposes is primordial. We expect their composition to closely reflect the solar system distribution of the elements. The solar EUV radiation below 3000Å can get down as deep as approximately the 1 bar level on these planets. Absorption of this radiation by species such as ammonia, methane, phosphine, etc. leads to a photochemical sequence of reactions which not only alter the distribution of the parents, but result in the formation of numerous products. Thermodynamic considerations lead to the formation of various clouds such as those of ammonia, ammonium hydrosulfide, water, methane, ethane, and acetylene. A clear case of coupling between the equilibrium thermochemistry and disequilibrating processes, such as photochemistry, is seen in the case of Uranus. Table 1 summarizes the species in the outer planets which undergo photochemical transformation and/or condensation. This chapter presents a discussion of these processes in the atmospheres of Jupiter, Saturn and Uranus.

TABLE 1

SPECIES PARTICIPATING IN PHOTOCHEMISTRY AND CONDENSATION AT TEMPERATURES BELOW 400K

Species[1]	Solar Ratio of Elements	Jupiter		Saturn		Uranus	
		Photo.[2]	Condens.[2]	Photo.	Condens.	Photo.	Condens.
H_2O	$O/H=6.8\times10^{-4}$	No	Yes	No	Yes	No	Yes
CH_4	$C/H=3.7\times10^{-4}$	Yes	No	Yes	No	Yes	Yes
C_2H_4		Yes	No	Yes	No	Yes	No
C_2H_6		Yes	No	Yes	No	Yes	Yes
C_2H_2		Yes	No	Yes	No	?	Yes
NH_3	$N/H=1.0\times10^{-4}$	Yes	Yes	Yes	Yes	No	Yes
N_2H_4		Yes	Yes	Yes	Yes	No	No
H_2S	$S/H=1.6\times10^{-5}$	?	Yes	No	Yes	No	Yes
PH_3	$P/H=3.0\times10^{-7}$	Yes	No	Yes	No	?	?
CH_3NH_2							
HCN							
CO							

1. Species marked with a parenthesis are products of photochemical reactions. H_2S might condense as NH_4SH.
2. Photo., Condens. mean participating in photochemistry and condensation, respectively. The role of species marked with a '?' is uncertain.

2 COMPOSITION AND STRUCTURE OF THE ATMOSPHERE

Photochemical calculations are dependent on the composition of the mixed atmosphere, temperature profile, vertical mixing, and the solar fluxes. For Jupiter and Saturn, most of the above information was obtained simultaneously on Voyagers 1 and 2 from measurements done with the radio science subsystem (RSS), infrared spectrometer (IRIS), ultraviolet spectrometer (UVS), and the imaging subsystem (ISS). Only very rudimentary knowledge of the atmospheric composition and the thermal structure of Uranus is available from some ground based infrared and microwave measurements. Figures 1 and 2 adapted from Atreya, et al. (1981) and Atreya, et al. (1984) show the measured composition and temperature profiles for Jupiter and Saturn.

Figure 1. Composition and thermal structure of the Jovian atmosphere. Altitudes shown are above the NH_3-cloud tops located at P=600 mb, T=150K (add approximately 15km to obtain altitudes above the 1-bar level). Pressures (right ordinate) correspond to the altitudes on the left ordinate. Broken line interpolations represent 'data gap' region in the middle atmosphere. Exospheric temperature of 1100K is reached at 1450 km. Data above 300 km are from α Leo UV stellar occultation; those below 150 km from IRIS and RSS. Adapted from Atreya, et al. (1981).

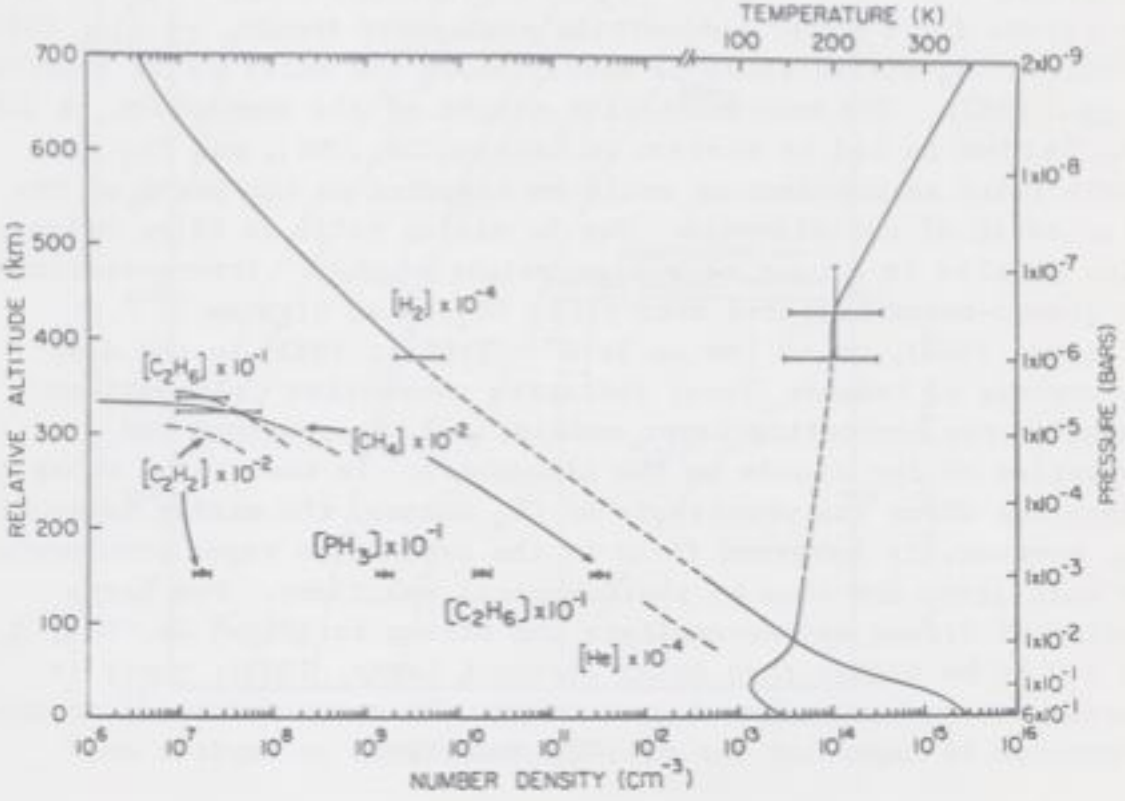

Figure 2. Composition and thermal structure of Saturn. Altitudes are above the 1-bar level. Adapted from Atreya, et al. (1984)

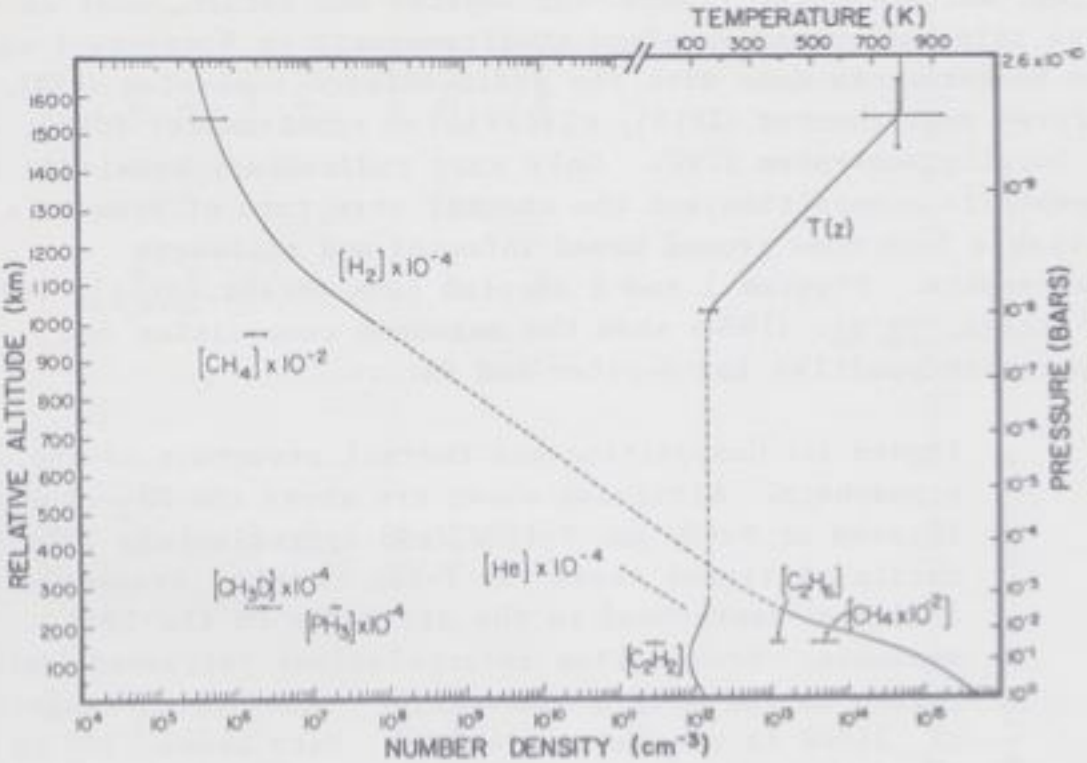

The mixing ratios of NH_3 and PH_3 on Jupiter are found to be close to the values for a solar composition atmosphere (Kunde, et al., 1982), while the CH_4 mixing ratio is nearly twice the solar value (Gautier, et al., 1982). The mean molecular weight of the homosphere is 2.2, i.e., helium is 11% by number. On Saturn, CH_4, NH_3, and PH_3 are nearly twice as abundant as would be expected on the basis of the solar ratio of the elements. The He mixing ratio is 6% by volume, which results in a mean molecular weight of 2.12. Interpretation of the ground-based infrared data yield CH_4/H_2 as high as 10^{-1} (Wallace, 1980), or as low as 3×10^{-3} (Teifel, 1983) in the deep troposphere of Uranus. These radiative convective calculations depend on the scattering layer models, and the presence and properties of the clouds in the atmosphere. In the region above the tropopause where the photolysis of CH_4 occurs, the mixing ratio of CH_4, however, is governed first by the saturation vapor pressure at the cold trap, and then by photochemical reactions. The large density of Uranus may necessitate the mixing ratios of He, NH_3, H_2S, and H_2O to be higher than solar (Prinn & Lewis, 1973); there is however no evidence of such enrichment. The temperature up to the tropopause is important for the NH_3 photolysis on Jupiter and

Saturn. Above the tropopause, however, only 'average' temperature is known until the homopause is reached (see Figs. 1 and 2). Small changes about the mean temperature do not terribly affect the photochemical results. The temperature at the inversion layer located somewhere between 10 and 200 mb on Uranus is found to be ~57K (Tokunaga, et al., 1983). The models of Wallace (1980) and Courtin, et al. (1978), however, can tolerate temperatures as low as 50K. For the inversion layer at 100mb, a 50K temperature would result in CH_4/H_2 of 2.4×10^{-5}, and 2.2×10^{-4} at 55K on the basis of the saturation vapor pressure curves of CH_4 (see Fig. 3 for the saturation vapor pressures of gases of interest in this chapter).

Figure 3. Saturation vapor pressures of various gases of interest in the outer planets. The inset is for the H_2O saturation vapor pressures at temperatures shown on the upper abscissa of the inset.

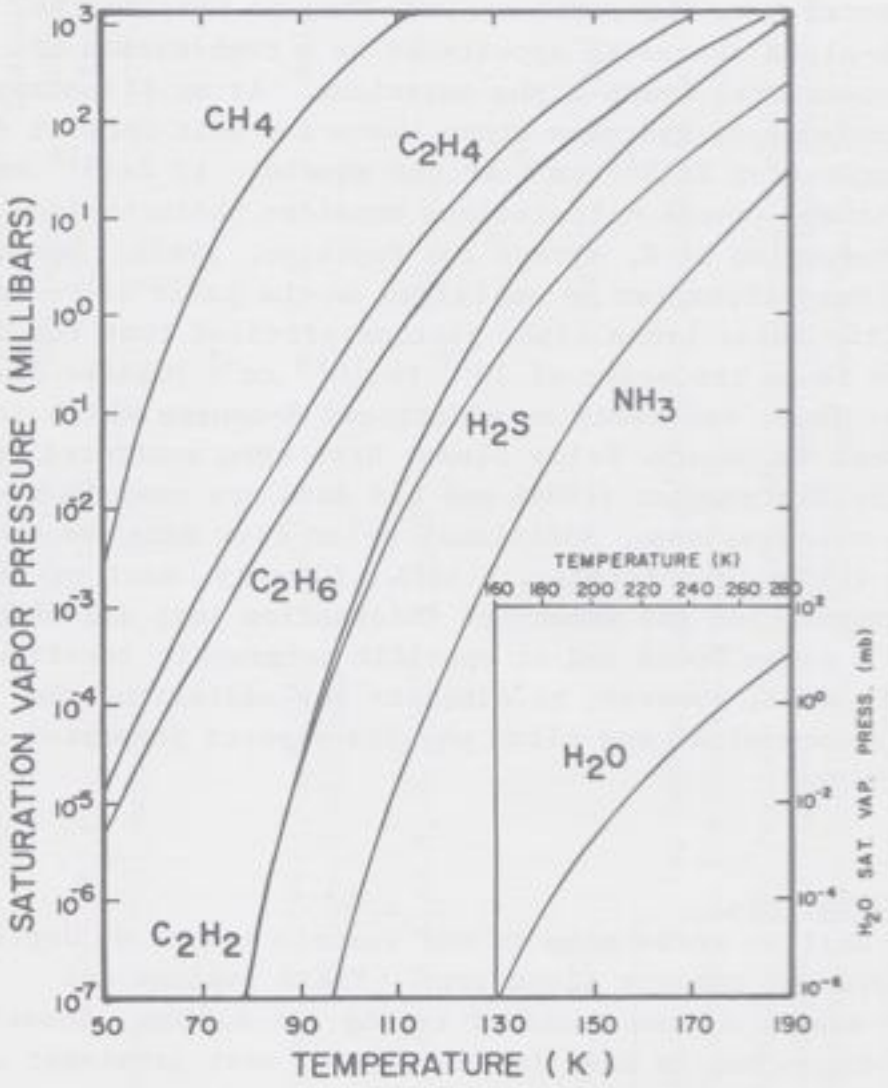

Vertical mixing in the region of photolysis has not been measured directly. However, measurements done near the homopause can be reasonably extrapolated to the troposphere with a $K \propto M^{-1/2}$ variation (Atreya, et al., 1981), where M represents the atmospheric number density. The relevant values of the eddy diffusion coefficient are given in Table 2. For Jupiter and Saturn, the values were derived from the analysis of the UV stellar occultation data. No such measurements are available for Uranus. Since Uranus does not possess an internal heat source (Lowenstein, et al., 1977), and that the globally averaged value of the auroral energy implied from the observed Lyman-alpha emission rates (Clarke, 1982) is less than 0.02 erg cm^{-2} s^{-1} (Atreya & Ponthieu, 1983), it is not expected to exhibit large vertical mixing. K_h on the order of 10^4 to 10^6 cm^2 s^{-1} at the homopause is conceivable. K_h as low as 10^4 cm^2 s^{-1}, however, has not been encountered on any planet. Note that unlike in the case of Jupiter and Saturn, one cannot arrive even at an order of magnitude estimate of K_h at Uranus from its Lyman alpha emission intensity measured from the earth orbit. This is because the measured Lyman-alpha intensity appears to be a combination of auroral and non-auroral Lyman-alpha emissions. As an illustration, the column abundance of hydrogen atoms above the unit optical depth in methane ranges from 2×10^{15} cm^{-2} at the equator to 2×10^{16} cm^{-2} in the polar latitudes (these calculations consider photochemical and ionospheric production of H, Atreya and Ponthieu, 1983). However, the observed Lyman-alpha can be explained on the basis of resonance scattering of the solar Lyman alpha photons provided that the H-column density is on the order of 10^{17} to 10^{18} cm^{-2} (Clarke & Atreya, 1983). Thus, one needs an additional H-source which is probably auroral in nature. Solar fluxes have been monitored on the AE satellite by Hinteregger (1981) and his data are used in most photochemical calculations. Additional solar flux data are taken from Ackerman (1971), and Rottman, (1981). Clearly, most of the atmospheric composition and structure information just discussed is applicable to a given epoch and at specific geographic location on the planet. It will, however, be adequate for addressing the fundamental photochemical and cloud physics aspects presented in the following sections.

3 AMMONIA (NH_3)

The whitish areas seen in the visible images of Jupiter and Saturn represent ammonia cloud tops. These regions are generally the zones, or the areas of rising air motion. Sometimes, an orange-red-brown hue is seen in the clouds, most prominent of

TABLE 2

EDDY DIFFUSION COEFFICIENT AND TEMPERATURE

	K_h ($cm^2\ s^{-1}$)	Density at[1] Homopause (cm^{-3})	Altitude of[2] Homopause (km)	Atmospheric Pressure at Homopause (bars)	Photolysis[3] Region Temperature (K)	References
Uranus	10^4-10^6 expected	?	?	10^{-6} to 10^{-7}	~100	Atreya & Ponthieu (1983); French, et al. (1983)
Saturn	$1.7(+4.3,-1.0)\times10^8$ $8.0(+4.0,-4.0)\times10^7$	1.2×10^{11}	1110	4×10^{-9}	140	Atreya (1982); Sandel, et al. (1982)
Jupiter	$1.4(+0.8,-0.7)\times10^6$	1.4×10^{13}	440	10^{-6}	170	Atreya, et al. (1981); McConnell, et al. (1982)
Earth	10^6	10^{13}	100	3×10^{-7}		Hunten (1975)

[1] Density: H_2 for Jupiter, Saturn and Uranus; atmospheric for others. Densities at the homopause correspond to the central values of K_h.

[2] Altitude: For Jupiter and Saturn, the altitudes are above the 1-bar atmospheric pressure level in the equatorial region; some previous publications had the cloud-tops or the 10^{19} cm^{-3} level as the reference. For Earth, the altitudes are above the surface.

[3] Temperature: Average temperature in the middle atmosphere photochemical regime is given. See text for temperature profile near the NH_3 and CH_4 clouds.

which is the Great Red Spot of Jupiter (GRS). The color may be caused by the presence of some chromophore, such as phosphorus, sulfur or polymers of hydrogen cyanide. Gas phase ammonia exists in the cloud regions of Jupiter and Saturn, and its abundance near the cloud tops is dictated by its saturation vapor pressure. Rayleigh scattering inhibits penetration of solar photons shortward of 2000Å below the 10^{19} cm^{-3} level. Solar photons between 1600 and 2300Å are responsible for decomposing ammonia at pressures lower than 600mb. In the presence of other Jovian gases, particularly H and H_2, a series of chemical reactions ensue, with the eventual products being N_2H_4 and N_2. On Uranus, NH_3 photolysis cannot occur since NH_3 is buried well below the CH_4 clouds where the solar photons of wavelengths 2000Å cannot reach (see Sec. 15). The chemical scheme for NH_3-photolysis on Jupiter and Saturn is presented in Table 3, and is illustrated in Fig. 4. The chemical scheme taken from Atreya, et al. (1977) is an improvement over the earlier work of Strobel (1973a). Following photodecomposition of NH_3, amidogen radicals (NH_2) are produced in the ground state. Some of the NH_3 is recycled immediately by the reaction of NH_2 with H (reaction R3.2). However, most of the NH_2 radicals undergo self-reaction forming hydrazine, N_2H_4 (R3.3). N_2H_4 molecules would condense at the temperatures prevalent in the Jovian and Saturnian tropospheres. This would eventually result in haze or snow of N_2H_4 in the tropospheres of these planets.

TABLE 3 AMMONIA PHOTOCHEMISTRY (Atreya, et al., 1977)

Chemical Reactions	Reaction Number
$NH_3+h\nu \longrightarrow NH_2(X)+H$	(R3.1)
$NH_2(X)+H \longrightarrow NH_3$	(R3.2)
$NH_2(X)+NH_2(X) \longrightarrow N_2H_4$	(R3.3)
$N_2H_4+H \longrightarrow N_2H_3+H_2$	(R3.4)
$N_2H_4+h\nu \longrightarrow N_2H_3+H$	(R3.5)
$N_2H_3+H \longrightarrow 2NH_2$	(R3.6)
$H+H+M \longrightarrow H_2+M$	(R3.7)
$N_2H_3+N_2H_3 \longrightarrow 2NH_3+N_2$	(R3.8)
$N_2H_3+N_2H_3 \longrightarrow N_2H_4+N_2H_2$ $\longrightarrow N_2H_4+N_2+H_2$	(R3.9)

Figure 4. Photochemistry of ammonia on Jupiter and Saturn. Adapted from Atreya, et al. (1978).

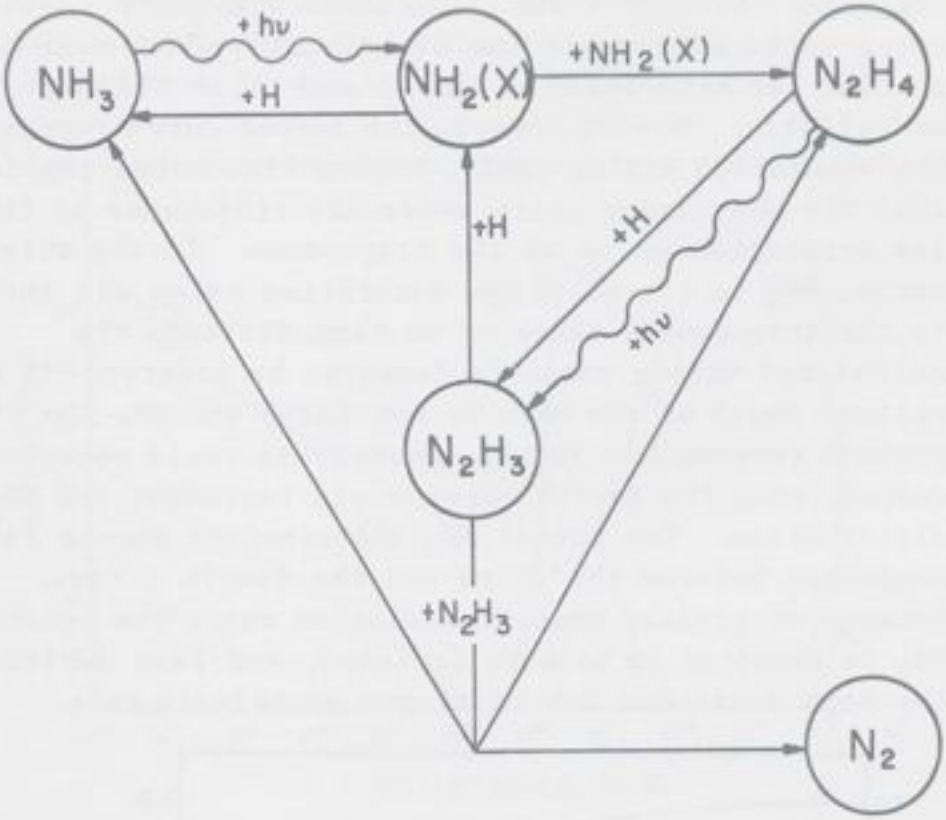

Both with and without supersaturation, N_2H_4 present in the gas phase would undergo photolysis (R3.5), and the hydrogen extraction reaction (R3.4). After several intermediate reactions (R3.6-R3.9), nitrogen (N_2) would be formed. The possible condensation of N_2H_3 is treated similar to that of N_2H_4. Shown in Fig. 5 is a typical distribution of NH_3 in the Jovian midlatitudes. These calculations were done by solving a set of non-linear partial differential equations representing one dimensional continuity equations in the steady state, as in Atreya, et al. (1977). Note in Fig. 5 that without saturation, NH_3 abundances are much greater after photolysis than in the case where NH_3 is forced back to its saturation value wherever the NH_3 partial pressure exceeds the saturation vapor pressure. Above the tropopause however, photochemistry and transport deplete NH_3 to well below its saturation limit. The actual photochemical distribution depends on the depth of penetration of the solar photons, which in turn can be influenced by the extent of atmospheric haze.

Figure 5. Typical midlatitude NH_3 distributions from photochemical considerations. Atmospheric densities on the right ordinate correspond to the heights on the left ordinate. Altitudes are taken above the 1-bar level. The outer curve represents the distribution which does not account for saturation of NH_3 -- and it is clearly unrealistic. Moving inward, the second curve represents the saturation mixing ratio, broken line curve implies that the NH_3 mixing ratio above the tropopause is fixed by its saturation value at the tropopause. In the third curve, NH_3 is forced to the saturation value all the way to the tropopause, since up to that altitude the calculated mixing ratio is found to be greater. If the optical depth of the haze is not large enough, the UV photons responsible for NH_3 photolysis could penetrate deeper, then the fourth curve would represent the NH_3 distribution. The actual NH_3 distribution should lie somewhere between the third and the fourth curves. Because of greater photodissociation rate, the equatorial NH_3 is expected to be more depleted, and less depleted in the high latitudes due to slower photolysis rate.

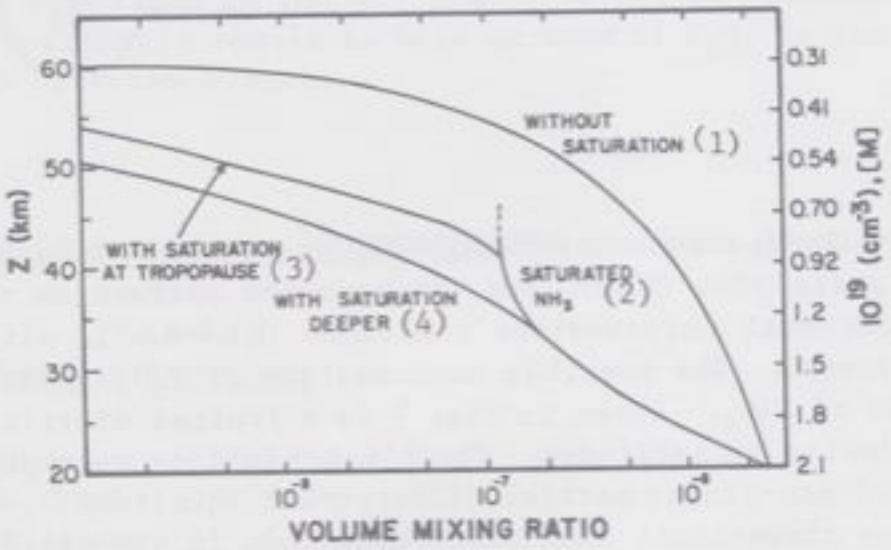

In the equatorial region the NH_3 abundances would be lower than shown in Fig. 5 due to the greater photolysis rates; the opposite would be true for the high latitudes. The distribution of the products of NH_3 photolysis is shown in Fig. 6. The maximum N_2 mixing ratio is calculated to be between 10^{-8} and 4×10^{-11} with and without supersaturation of N_2H_4 respectively. Prinn & Olaguer (1981) have proposed that vertical motions on Jupiter are large enough to transport large amounts of N_2 to the upper atmosphere.

Figure 6. Volume mixing ratios of the photochemical products of NH_3. Curves marked ----- for N_2H_4 and N_2H_3 assume saturation vapor mixing ratios for these species, i.e., no supersaturation is permitted. The resulting N_2 mixing ratio for this situation is marked by ----- N_2. Adapted from Atreya, et al. (1977).

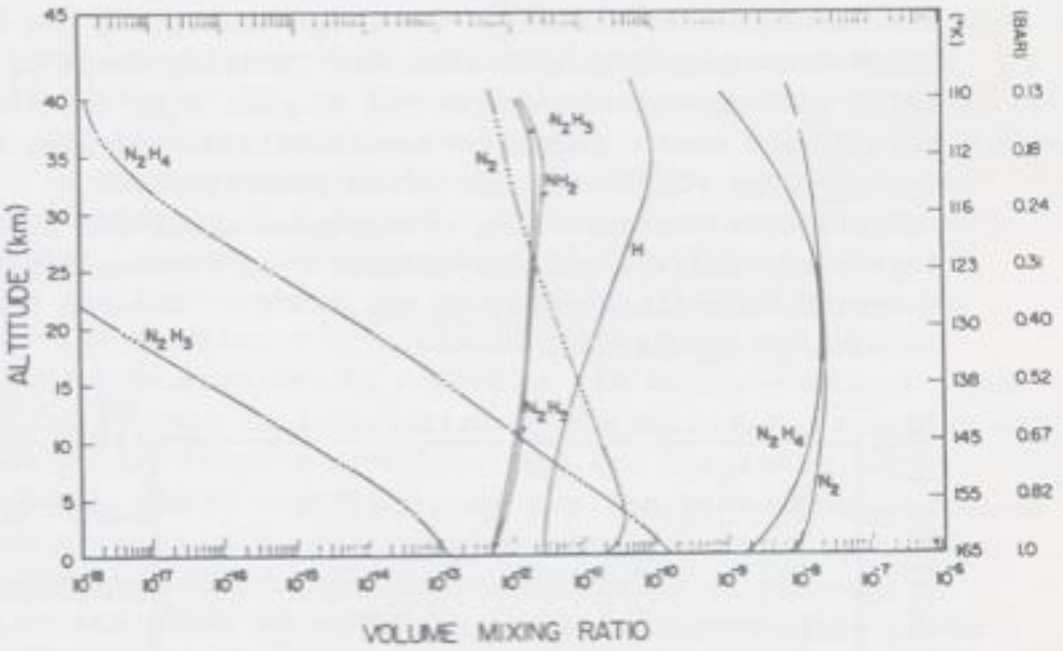

They predict N_2 mixing ratios of $(0.6\text{-}10)\times10^{-6}$. A test of whether N_2 is produced photochemically (Atreya, et al., 1977), or is upwelled from the interior (Prinn & Olaguer, 1981) will have to wait until after the data from the Galileo Probe Mass Spectrometer have been obtained, analyzed and interpreted in 1989. Photochemical calculations for NH_3 on Saturn done in the same manner as for Jupiter are shown in Fig. 7. Again, there is a distinct possibility of N_2H_4 haze formation on Saturn as well.

4 PHOSPHINE (PH_3)

PH_3 is thermochemically stable below the 800K level in the deep atmosphere of Jupiter. Between 800 and 300K, PH_3 can be oxidized to P_4O_6 by H_2O. Above the 300K level, P_4O_6 would dissolve in H_2O. However, PH_3 has been detected in the troposphere and stratosphere of Jupiter and Saturn (Ridgway, et al., 1976; Larson, et al., 1977; Beer & Taylor, 1979; Kunde, et al., 1982; Hanel, et al., 1981). Prinn & Lewis (1975) have argued that strong vertical mixing can transport PH_3 faster to the upper atmosphere than the

Figure 7. Typical midlatitude distribution of NH_3, NH_2, and N_2 above the cloud tops of Saturn. The NH_3 curve marked 'S' refers to the saturation mixing ratio, and represents the minimum NH_3 mixing ratio profile. A small degree of supersaturation is allowed in the broken line curve ($K_o = 2\times10^3$ cm^2 s^{-1} and $K \propto 1/\sqrt{M}$) and the dotted curve ($K_o = 10^4$ cm^2 s^{-1} and constant). N_2H_4 mixing ratios are smaller than 1.3×10^{-9}. Rayleigh scattering has been taken into consideration. The two limiting cases of N_2 refer to: no supersaturation of NH_3 and N_2H_4 (dot-dashed curve), and small degree of supersaturation (broken line curve). The right ordinate gives densities and temperatures corresponding to altitudes above the cloud tops (left scale), and are deduced from Pioneer/Saturn infrared data (Ingersoll, et al., 1980). Adapted from Atreya, et al. (1980).

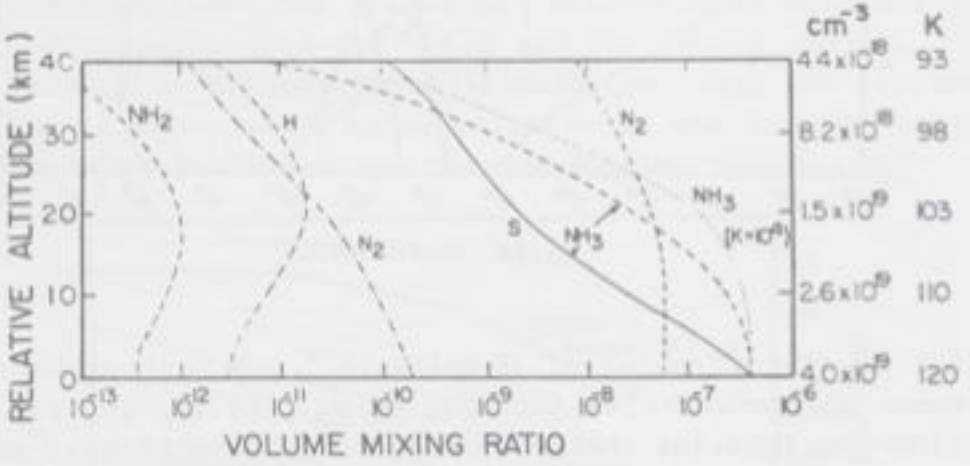

time coustant for the oxidation of PH_3 to P_4O_6. The latter is estimated to be 6 days, with $K=10^9$ cm^2 s^{-1} (Prinn & Owen, 1976). Once above the ammonia cloud tops, PH_3 undergoes photolysis above the 80 mb level following absorption of the solar photons between 1600 and 2350Å, i.e., in essentially the same wavelength range as NH_3. The chemical scheme for the PH_3 photolysis is shown in Table 4. Unlike NH_3, PH_3 is not recycled by ($H+PH_2$) reaction. The final product of this scheme is triclinic red phosphorus. These phosphorus crystals can provide the reddish coloration seen in the GRS and the other clouds provided that the density of $P_4(s)$ is large enough for about unit optical depth in the visible. $K \simeq 10^6$ cm^2 s^{-1} throughout The upper troposphere and the interior would be required for $\tau_{P_4} = 1$ (Prinn & Lewis, 1975). $K \simeq 10^6$ has been measured only near the homopause (Atreya, et al., 1981), which implies a relatively low value of 5×10^2 to 10^3 cm^2 s^{-1} for K near the tropopause. Indeed,

the variation of K from $5x10^2$ at the tropopause to 10^6 at the homopause gives best fit to the observed hydrocarbons in the upper atmosphere (Atreya, et al., 1981). In the GRS region, however, K could be greater, as suggested by Prinn & Lewis (1975).

Vera-Ruiz & Rowland (1978) have shown from their laboratory measurements that C_2H_2 and C_2H_4 act as efficient scavengers of PH, P_2 and PH_2, thus suppressing the formation of the $P_4(s)$ crystals. As in Prinn and Lewis, they have suggested that strong vertical mixing could transport PH_3 to the upper atmosphere where it would be photolyzed, and thus prevent the scavenging action of C_2H_2 and C_2H_4. The Voyager IR measurements (Kunde, et al., 1982), however, give fairly high abundances of C_2H_2 and C_2H_4 (which are consistent with the proportions taken in the experiment of Vera-Ruiz & Rowland) precisely in the region where the photolysis of PH_3 occurs. The formation of red phosphorus crystals is thus questionable. An important caveat to consider in regard to the measurements of Vera-Ruiz & Rowland is that no information on the activation energies at the relevant Jovian temperatures (150-110K) are available for reactions (R4.2), (R4.4) and (R4.5), or for the scavenging reactions of the phosphorus species which compete with reactions R4.2, R4.4 and R4.5. Another complication in the formation of the red phosphorus crystals may arise due to possible intermediate product, diphosphine P_2H_4, in the PH_3 photochemical scheme. Ferris & Benson (1980) have found that absorption of 2062Å photons by PH_3 yielded P_2H_4 as an intermediate product on the path to P_4 formation.

TABLE 4 PHOTOCHEMISTRY OF PH_3 (Prinn & Lewis, 1975)

Chemical Reactions	Reaction Number
$PH_3 + h\nu \longrightarrow PH_2 + H$	(R4.1)
$PH_2 + PH_2 \longrightarrow PH + PH_3$	(R4.2)
$PH_3 + H \longrightarrow PH_2 + H_2$	(R4.3)
$PH + PH \longrightarrow P_2 + H_2$	(R4.4)
$P_2 + P_2 \longrightarrow P_4(g)$	(R4.5)
$P_4(g) \longrightarrow P_4(s)$	(R4.6)
$H + H + M \longrightarrow H_2 + M$	(R4.7)

R4.3 may compete with R4.7 at high temperatures.

The yield of P_2H_4 rises to a maximum in about 5 hours of illumination time, and then drops to 20% of the maximum. The chemical scheme they suggested following the reaction R4.1 ($PH_3+h\nu \rightarrow PH_2+H$) is similar to the one for NH_3 (see Table 3), and is presented in Table 5. It should be emphasized that the experiment was done at room temperature which is considerably higher than the 150-110K range in the Jovian atmosphere. No reliable thermodynamical data on P_2H_4 are available at the relevant Jovian temperatures. However, if P_2H_4 behaves at all like N_2H_4, it is surely going to condense out, and the abundance of P_4 will be reduced drastically. Moreover, unlike the Jovian atmosphere, no excess of H_2 was allowed in the laboratory mixture.

TABLE 5 PHOTOCHEMISTRY OF PH_3
(According to Ferris & Benson, 1980)

Chemical Reactions	Reaction Number
$PH_3 + h\nu \longrightarrow PH_2 + H$	(R4.8)
$PH_2 + PH_2 \longrightarrow P_2H_4$	(R4.9)
$P_2H_4 + H \longrightarrow P_2H_3 + H_2$	(R4.10)
$P_2H_4 + PH_2 \longrightarrow P_2H_3 + PH_3$	(R4.11)
$P_2H_3 + H \longrightarrow P_2H_2 + H_2$	(R4.12)
$P_2H_3 + P_2H_3 \longrightarrow P_2H_2 + P_2H_4$	(R4.13)
$P_2H_3 + PH_2 \longrightarrow P_2H_2 + PH_3$	(R4.14)
$P_2H_2 + h\nu \longrightarrow P_2 + H_2$	(R4.15)
$P_2 + P_2 \longrightarrow P_4(g) \longrightarrow P_4(s)$	(R4.16)
$H + H + M \longrightarrow H_2 + M$	(R4.17)

TABLE 6 NH_3-PH_3 COUPLING

Chemical Scheme	Reaction Number
$NH_3 + h\nu \longrightarrow NH_2 + H$	(R5.1)
$NH_2 + NH_2 \longrightarrow N_2H_4$	(R5.2)
$NH_2 + PH_3 \longrightarrow NH_3 + PH_2$	(R5.3)
$PH_3 + H \longrightarrow PH_2 + H_2$	(R5.4)

5 NH_3-PH_3 COUPLING, AND NH_3 RECYCLING

Strobel (1977) had suggested that the abundances of both PH_3 and NH_3 could be altered due to the possible coupling between the two photochemistries. In particular, the sequence of reactions listed in Table 6 is involved. In the NH_3 photochemical scheme (Table 3), NH_2 self-reaction (reaction R5.2) produces N_2H_4. However, it could compete with its reaction with PH_3 to recycle NH_3 (R5.3 above). In the Jovian atmosphere, this mechanism of recycling would be important if the rates of reaction R5.3 and R5.4 are comparable. Recent laboratory measurements by Bosco, et al. (1983) have shown that the rate constant for reaction R5.3, $k_3=3.2\times10^{-15}$ at 150K, which is 10^{-5} of the rate constant for self-reaction of NH_2 (Reaction R5.2). Moreover,

$$k_3 = 10^{-2}\, k_4$$

Hence, not only reaction R5.3 does not recycle NH_3, but that the coupling between NH_3 and PH_3 photochemistries is of insignificant importance. Since PH_3 mixing ratio at all altitudes in the photochemical regime is much lower than the NH_3 mixing ratio, even the solar photons in the NH_3 photolysis are not attenuated by PH_3.

Photochemical reactions of NH_3 listed in Table 3 can irreversibly destroy NH_3 in less than 60 My on Jupiter. Ammonia, however, maintains the same mixing ratio as expected for a solar composition atmosphere. Since NH_3 is not recycled by $NH_2 + PH_3 \rightarrow NH_3 + PH_2$ reaction, the mechanisms suggested earlier (Strobel, 1973a, and Atreya & Donahue 1979) are still plausible. These involve snow-out, and subsequent mixing of N_2H_4 to the deep hot interior of Jupiter and Saturn, where N_2H_4 would be thermally dissociated to NH_2. At those high temperatures and pressures, NH_2 can react with H_2 to produce NH_3. NH_3 would, in turn, convect to the troposphere. The chemical scheme is summarized below:

$$N_2H_4 \xrightarrow{\text{high T}} NH_2 + NH_2 \qquad \text{(R5.5)}$$

$$2NH_2 + H_2 \longrightarrow 2NH_3 \qquad \text{(R5.6)}$$

Another possibility is the reaction of N_2 with H_2, again in the hot interior at pressures of 3000 bars.

$$N_2 + 3H_2 \longrightarrow 2NH_3 \qquad \text{(R5.7)}$$

None of the above reactions occur in the cold tropospheres where the temperatures and pressures are low, and activation energies high.

6. Methane (CH_4)

Photochemistry of methane has been discussed extensively by Strobel (1969, 1973b, and 1975). Further improvements and modifications were carried out by Atreya, et al. (1981); Atreya (1982); and Gladstone (1982). Methane is photolyzed below 1600Å resulting eventually in the formation of ethylene (C_2H_4), ethane (C_2H_6) and acetylene (C_2H_2) which are the stable non-equilibrium hydrocarbons. Further chemical reactions are conceivable so that higher order hydrocarbons such as propane, butane, methylacetylene, etc. are formed. The photochemical scheme for CH_4 in the atmosphere of the outer planets is shown in Fig. 8. Major pathways of the chemical reactions are presented in Table 7; a complete list of reactions and associated rate constants is given in Gladstone (1982).

Figure 8. Photochemical scheme for CH_4 in the atmospheres of major planets.

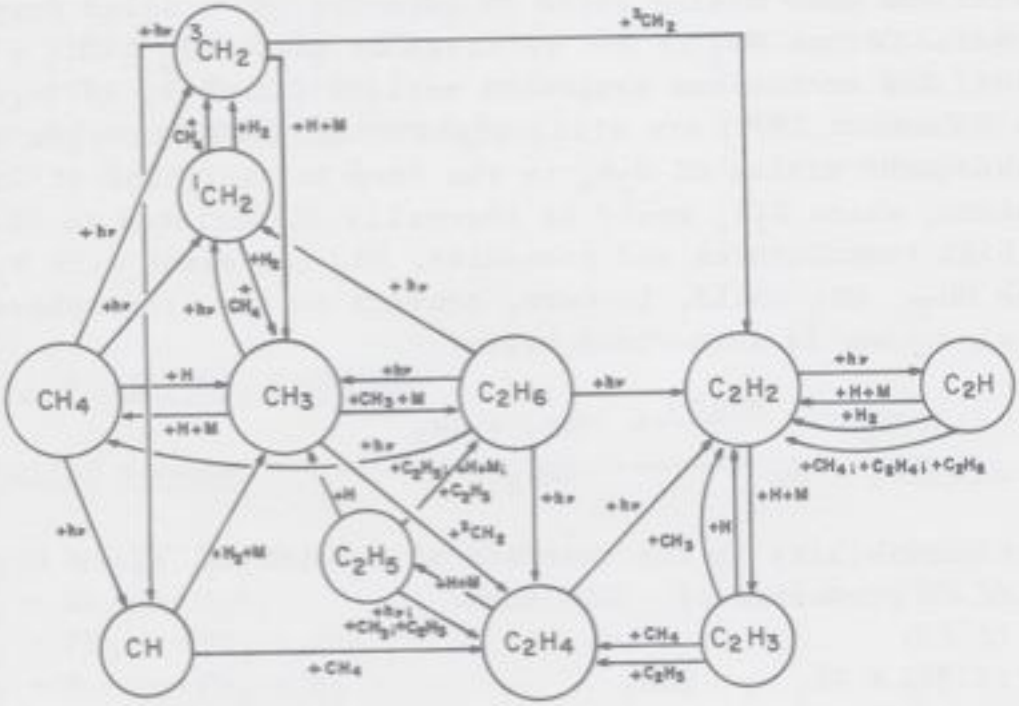

TABLE 7 CH_4 PHOTOCHEMISTRY (after Gladstone, 1982)

1. CH_4 is photolyzed in the upper layers (max. J at Lyα) and C_2H_4 is eventually produced (10% of all photons by CH_4 produce C_2H_4)

		Reaction Number
	$CH_4 + h\nu \longrightarrow {}^3CH_2 + 2H$	(R6.1)
	$CH_4 + h\nu \longrightarrow {}^1CH_2 + H_2$	(R6.2)
	${}^1CH_2 + H_2 \longrightarrow CH_3 + H$	(R6.3)
	$CH_3 + {}^3CH_2 \longrightarrow C_2H_4 + H$	(R6.4)
Net	$2CH_4 + 2h\nu \longrightarrow C_2H_4 + 4H$	(R6.5)
And		
	$CH_4 + h\nu \longrightarrow CH + H + H_2$	(R6.6)
	$CH + CH_4 \longrightarrow C_2H_4 + H$	(R6.7)
Net	$2CH_4 + h\nu \longrightarrow C_2H_4 + 2H + H_2$	(R6.8)

2. C_2H_4 is quickly lost by photolysis to C_2H_2, or by recycling to CH_4.

	$C_2H_4 + h\nu \longrightarrow C_2H_2 + H_2$	(R6.9)
	$C_2H_4 + h\nu \longrightarrow C_2H_2 + 2H$	(R6.10)
Net	$2(C_2H_4 + h\nu) \longrightarrow 2C_2H_2 + H_2 + 2H$	(R6.11)
And		
	$C_2H_4 + H + M \longrightarrow C_2H_5 + M$	(R6.12)
	$C_2H_5 + H \longrightarrow 2CH_3$	(R6.13)
	$2(CH_3 + H + M \longrightarrow CH_4 + M)$	(R6.14)
Net	$C_2H_4 + 4H \longrightarrow 2CH_4$	(R6.15)

3. Dissociation of CH_4 also leads to the formation of C_2H_6 (20% of all photons absorbed by CH_4 produce C_2H_6)

	$2(CH_4 + h\nu \longrightarrow {}^1CH_2 + H_2)$	(R6.16)
	$2({}^1CH_2 + H_2 \longrightarrow CH_3 + H)$	(R6.17)
	$2CH_3 + M \longrightarrow C_2H_6 + M$	(R6.18)
Net	$2(CH_4 + h\nu \longrightarrow C_2H_6 + 2H)$	(R6.19)

4. C_2H_6 is also lost by conversion to C_2H_2 or by recycling to CH_4, as is the case with C_2H_4

$$C_2H_6 + h\nu \longrightarrow C_2H_2 + 2H_2 \quad \text{(R6.20)}$$
$$C_2H_6 + h\nu \longrightarrow C_2H_4 + H_2 \quad \text{(R6.21)}$$
$$C_2H_6 + h\nu \longrightarrow C_2H_4 + 2H \quad \text{(R6.22)}$$

Followed by

$$C_2H_4 + h\nu \longrightarrow C_2H_2 + H_2 \quad \text{(R6.23)}$$
$$C_2H_4 + h\nu \longrightarrow C_2H_2 + 2H \quad \text{(R6.24)}$$

Net $$3C_2H_6 + h\nu \longrightarrow 3(C_2H_2) + 4H_2 + 4H \quad \text{(R6.25)}$$

And

$$C_2H_6 + h\nu \longrightarrow C_2H_4 + H_2 \quad \text{(R6.26)}$$
$$\longrightarrow C_2H_4 + 2H$$

Followed by

$$C_2H_4 \longrightarrow CH_4 \text{ Conversion, (R6.15)} \quad \text{(R6.27)}$$

$J_{C_2H_6} \leq 1/10\, J_{C_2H_4}$ so that C_2H_6 is stable in the upper atmosphere and is lost by diffusion to the lower altitudes.

5. Once produced in the above manner, C_2H_2 is highly stable; it undergoes the following reactions

$$H + C_2H_2 + M \longrightarrow C_2H_3 + M \quad \text{(R6.28)}$$
$$C_2H_3 + H \longrightarrow C_2H_2 + H_2 \quad \text{(R6.29)}$$

Net $$2H \longrightarrow H_2 \quad \text{(R6.30)}$$

And

6. $$C_2H_2 + h\nu \longrightarrow C_2H + H \quad \text{(R6.31)}$$
$$C_2H + H_2 \longrightarrow C_2H_2 + H \quad \text{(R6.32)}$$

Net $$H_2 \longrightarrow 2H \quad \text{(R6.33)}$$

C_2H_2 is therefore long-lived and its concentration builds up until its production is balanced by diffusive flux to the lower boundary. In the lower atmosphere also C_2H_2 is photolyzed and immediately recycled in the upper layer.

$C_2H_2 + h\nu \longrightarrow C_2H + H$ (R6.34)

$C_2H + CH_4 \longrightarrow C_2H_2 + CH_3$ (R6.35)

Net $CH_4 + h\nu \longrightarrow CH_3 + H$ (R6.36)

This is an indirect manner in which CH_4 can be 'dissociated' to give $CH_3 + H$. The reaction $CH_4 + h\nu \rightarrow CH_3 + H$ is not permitted (Slanger, 1982). CH_3 so produced, however, is either recycled to methane ($CH_3 + H + M \rightarrow CH_4 + M$) 65% of the time, or converted to ethane ($CH_3 + CH_3 + M \rightarrow C_2H_6 + M$) 35% of the time. Finally, higher order hydrocarbons, such as propane (C_3H_8), methylacetylene (C_3H_4), butane (C_4H_{10}), etc. are formed by reactions of the following nature:

$C_2H_5 + CH_3 + M \rightarrow C_3H_8 + M$ (R6.37)

$C_3H_7 + CH_3 + M \rightarrow C_4H_{10} + M$ (R6.38)

The heavier hydrocarbons diffuse down, some condense and snow out of the atmosphere. Once in the high pressure, high temperature interior of Jupiter and Saturn, they undergo pyrolysis and are decomposed to give CH_4. Methane is thus recycled, and it convects to the upper atmosphere.

The methane photolysis program of Atreya, et al. (1981) satisfactorily reproduces the UV stellar occultation data on CH_4, C_2H_2, and C_2H_6 in the upper atmosphere of Jupiter (Festou, et al., 1981). This program assumes values of K between 5×10^2 and 10^3 cm^2 s^{-1} at 10^{19} cm^{-3} level, and varying as $M^{-1/2}$ (where M=atmospheric density) to a value of 10^6 cm^2 s^{-1} at the homopause, where $M=10^{13}$ cm^{-3}. For Saturn, Atreya (1982) finds that the best fit to the hydrocarbon data (Festou and Atreya, 1982) requires $K=10^4$ cm^2 s^{-1} at 10^{19} cm^{-3} density level. Gladstone (1982) finds that his latest model for Jupiter yields hydrocarbon densities very similar to those of the stellar occultation data near the homopause, and in essential agreement with Atreya, et al. (1981) CH_4 photochemistry model results. Gladstone's CH_4 mixing ratio in the homosphere is somewhat higher than solar. A complete distribution of CH_4 photolysis products is shown for Jupiter in Fig. 9 (taken from Gladstone, 1982), and for Saturn in Fig. 10 (taken from Waite, Atreya, and Cravens, 1983).

Figure 9. Calculated distributions of CH_4 and its photochemical products on Jupiter. The height scale is the same as in Fig. 1.

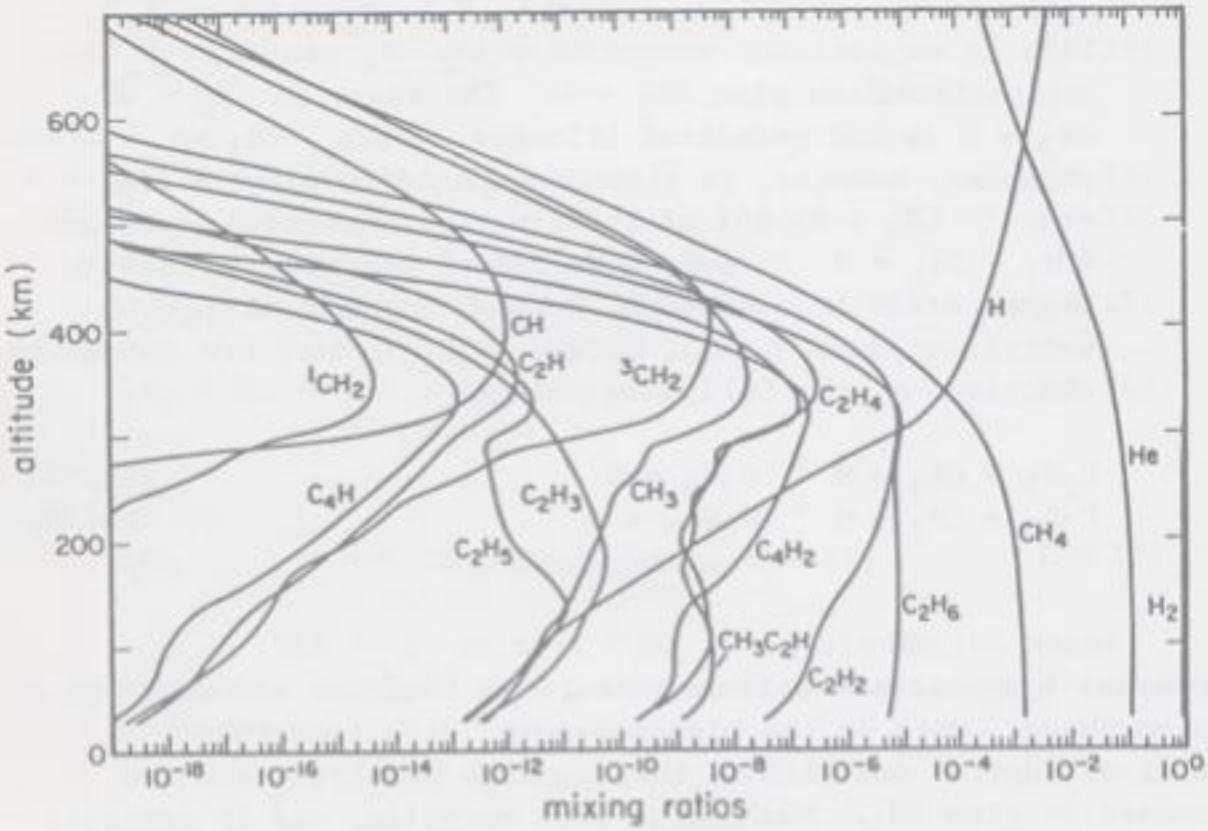

Figure 10. Calculated distributions of CH_4 and its photochemical products on Saturn. The height scale is same as in Fig. 2.

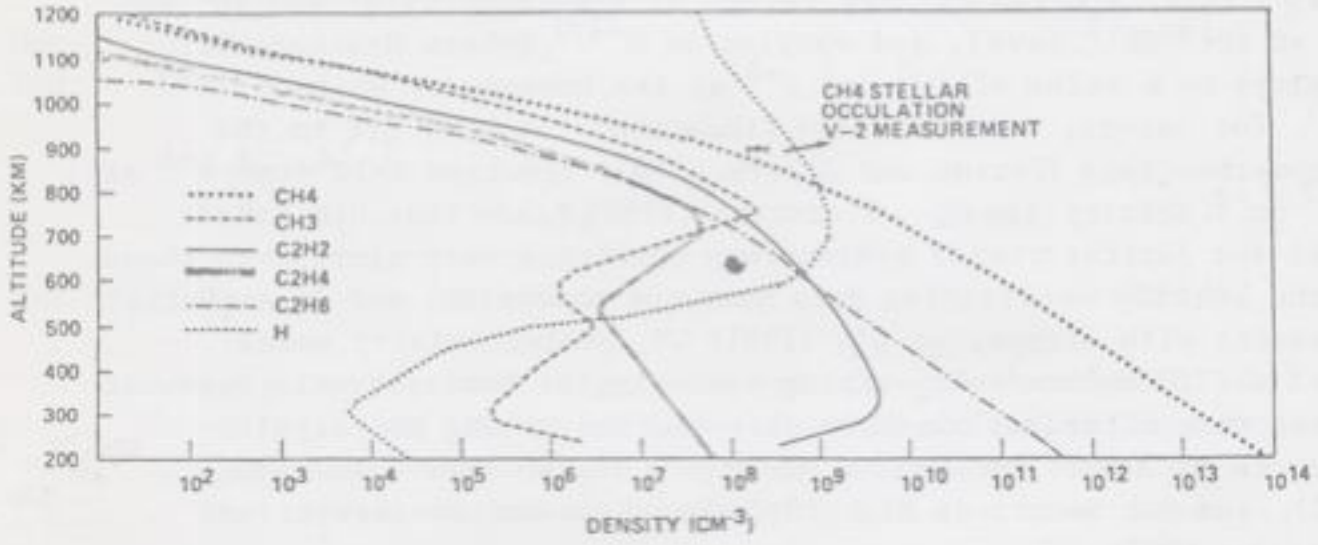

The results of recent methane photochemical calculations for Uranus by Atreya and Ponthieu (1983) are shown in Figs. 11 and 12.

Figure 11. Variation of CH_4 volume mixing ratio on Uranus with: (i) K_h: curves 'a', 'b', and 'c', where K_h=1.3x10^{10} cm^2 s^{-1}, 1.4x10^6 cm^2 s^{-1}, and 1.3x10^4 cm^2 s^{-1} respectively. Curves 'a', 'b', and 'c' have inversion temperature, T_{inv}=55K (P=100 mb; CH_4/H_2=2.4x10^{-4}), photolysis region temperature T_{photo}=95K, and latitude 2°. Curve 'b' is termed as the 'nominal' case; (ii) T_{inv}: curve 'd', where T_{inv}=50K so that $[CH_4]/[H_2]$=2.2x10^{-5} at the 100mb level. Other parameters are same as in curve 'b'; and (iii) latitude: curve 'e', where the latitude is 82° which represents the sub-solar point; the North-pole is pointing almost directly at the Sun in this geometry, and other parameters are same as in curve 'b'. The atmospheric densities shown on the right ordinate correspond to the altitudes on the left. Altitudes are referenced to the 100 mb (inversion layer) level. Add approximately 100 km to obtain altitudes above the 1-bar level (after Atreya and Ponthieu, 1983).

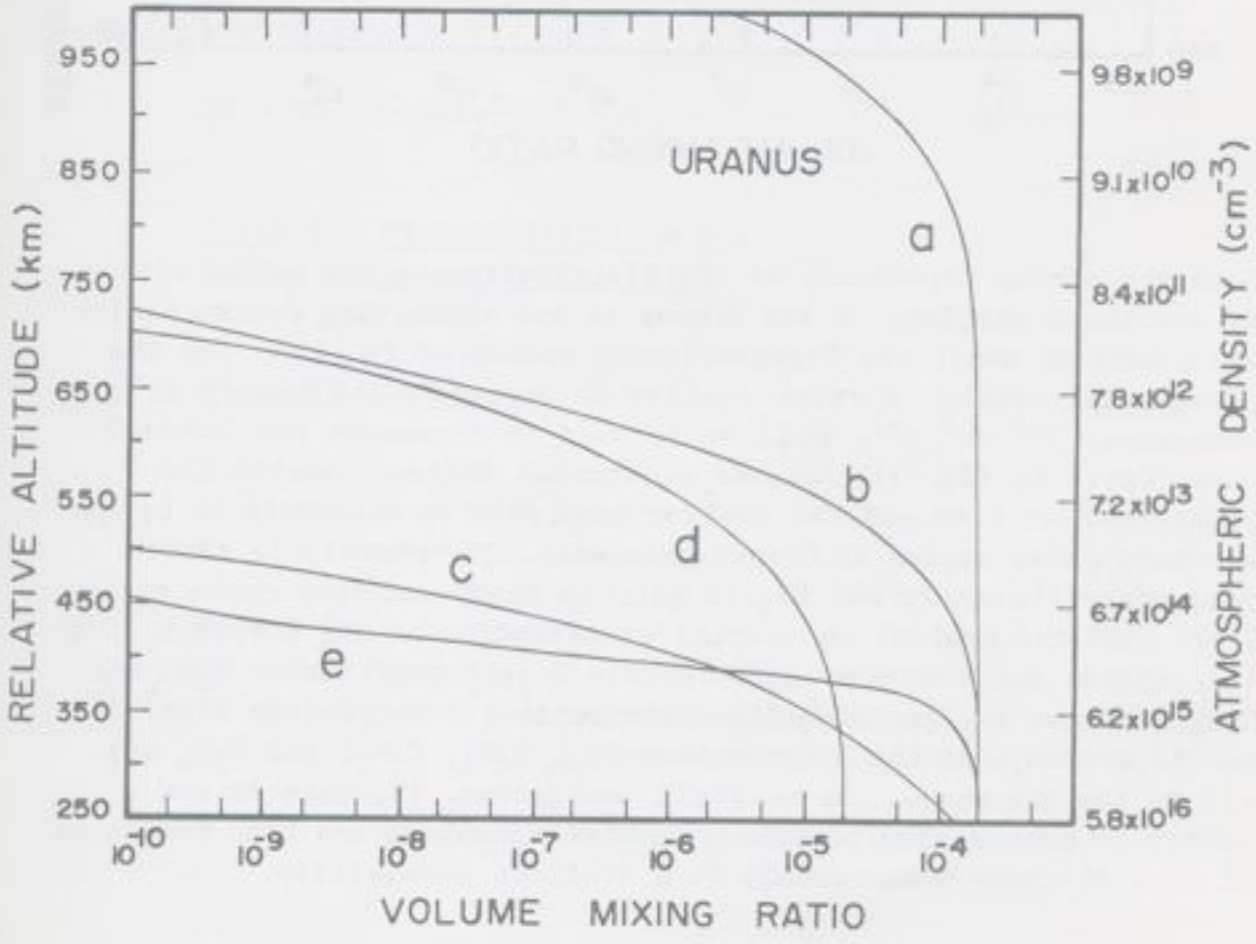

Figure 12. Volume mixing ratios of CH_4, C_2H_2 and C_2H_6 as a function of altitude (left ordinate) for the 'nominal' case. Here, eddy mixing coefficient at the tropopause, $K_o=10^3$ cm^2 s^{-1}, at the homopause, $K_h=1.4\times10^6$ cm^2 s^{-1}; temperature at the inversion level, $T_{inv}=55$K, in the photolysis regime, $T_{photo}=95$K; latitude=2°; and solar minimum flux. The atmospheric densities (right ordinate) correspond to the altitudes shown on the left coordinate. Altitude and density scales are same as in Fig. 11. (After Atreya and Ponthieu, 1983).

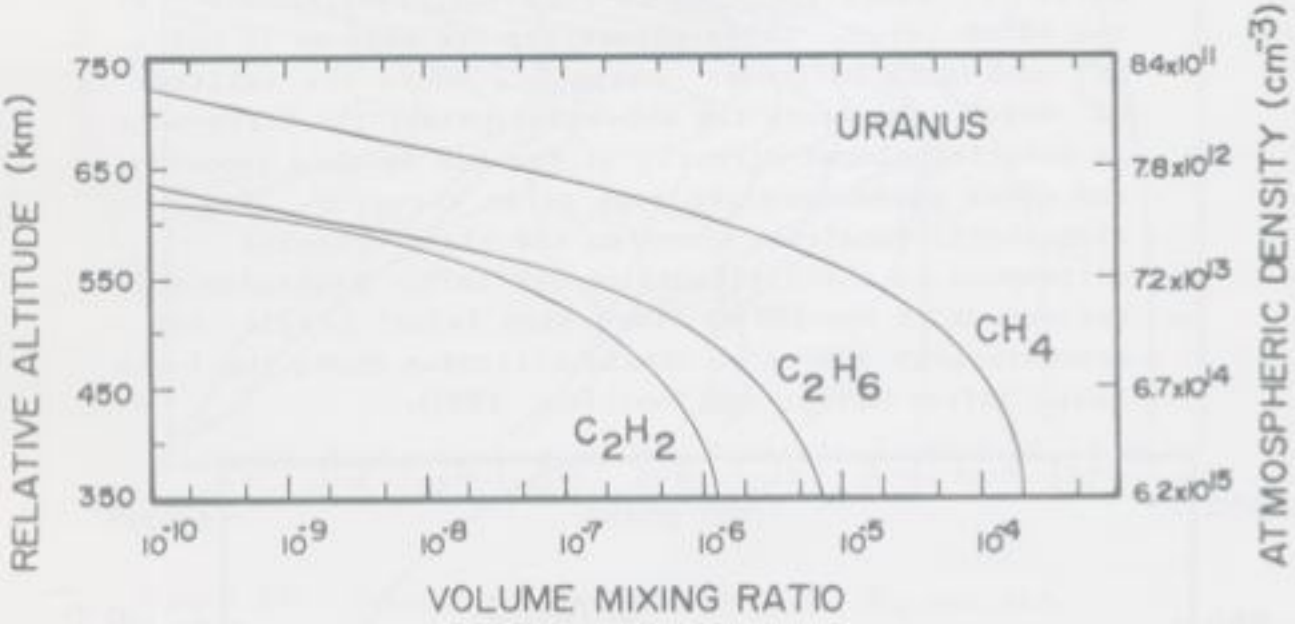

Note the strong dependence of CH_4 distribution on the value of K. As mentioned earlier, K for Uranus is not known, its determination will have to await the Voyager/Uranus encounter in 1986. For the present discussion, a value similar to Jupiter's and Earth's at the homopause, 10^6 cm^2 s^{-1}, will be assumed to represent the 'nominal' case (Curve b, Fig. 11) for the equatorial region. Due to the greater solar flux and the smaller mass path to attenuate it in the northern polar region of Uranus presently, CH_4 photolysis there proceeds efficiently and CH_4 is quickly destroyed (see curve e, Fig. 11). With the nominal equatorial distribution of CH_4 (curve b, Fig. 11), Atreya and Ponthieu (1983) obtain height profiles of C_2H_2 and C_2H_6 as shown in Fig. 12. The distributions presented in Figs. 11 and 12 assume that the hydrocarbons CH_4, C_2H_4, C_2H_2, and C_2H_6 are all in the gas phase. As we shall see in Sec. 15, this is not likely to be the case on Uranus, and condensation and haze formation of most of these hydrocarbons is a distinct possibility.

7. Hydrogen Sulfide (H_2S)

H_2S has not been detected on any of the major planets. This is perhaps because H_2S might condense as ammonium hydrosulfide (NH_4SH) at around 230K, and not be available above the NH_3 clouds. If H_2S undergoes photolysis, it does so by absorption of the solar photons shortward of 2700Å. Rayleigh scattering prevents photons shortward of 3000Å from penetrating below the 1-bar level. Photochemical scheme of H_2S is presented in Table 8.

The major photolysis products are HS and sulfur (S and S_2). Lewis and Prinn (1970) suggest that both S and S_2 would eventually be converted to elemental sulfur (S_8), ammonium polysulfide [$(NH_4)_xS_y$], and hydrogen polysulfides (H_xS_y) which are respectively yellow, orange and brown in color. It is further suggested that the coloration in relatively clear regions, such as the North Equatorial Belt (NEB) may be caused by the photolysis of H_2S, since the solar photons can penetrate to the region where H_2S may be found in sufficient quantities. The complete non detection of H_2S on the Jovian planets, is, however, puzzling and would imply that it does not escape condensation as NH_4SH. Moreover, laboratory measurements of Fowles, et al. (1967) indicate that at relatively high pressures ($P \gtrsim 0.5$ atm), the following self-reaction between HS might compete with R7.3 and R7.4:

$$HS + HS \rightarrow H_2S_2^* \rightarrow H_2S_2 \qquad (R7.10)$$

TABLE 8 PHOTOCHEMISTRY OF H_2S
(After Lewis and Prinn, 1970)

Chemical Reactions	Reaction Number
$H_2S + h\nu \longrightarrow HS + H$	(R7.1)
$+ H \longrightarrow HS + H_2$	(R7.2)
$HS + HS \longrightarrow H_2S + S$	(R7.3)
$H_2 + S_2$	(R7.4)
$HS + H + M \longrightarrow H_2S + M$	(R7.5)
$HS + H \longrightarrow H_2 + S$	(R7.6)
S and $S_2 \longrightarrow S_8$ (elemental sulfur, yellow)	(R7.7)
$(NH_4)_xS_y$ (ammonium polysulfides, orange)	(R7.8)
$\longrightarrow H_xS_y$ (hydrogen polysulfides, brown)	(R7.9)

Collisional deactivation of $H_2S_2^*$ is not very effective for P≤10 mb. Thus, the resulting product could be H_2S_2, and not sulfur. Pulse radiolysis of H_2S, on the other hand, yields S_2 via the following reaction:

$$H_2S + S \rightarrow H_2S_2^* \rightarrow H_2 + S_2 \qquad (R7.11)$$

The role of H_2S in the formation of sulfur in the Jovian atmosphere is thus questionable. It appears that at low pressures (P≃1 mb), the scheme given in Table 8 is operative, and sulfur would be formed. This would, however, necessitate presence of H_2S in the upper atmosphere where it has not been detected. Direct condensation of H_2S is unlikely since its saturation mixing ratio at even the tropopause temperature of Jupiter is a factor of three greater than its mixing ratio based on the solar abundance of sulfur.

8 C-N COUPLING: METHYLAMINE (CH_3NH_2)

Kuhn, et al. (1977) proposed that coupling between the photochemistries of ammonia and methane occurs in a narrow altitude region where the concentrations of CH_3 radicals and NH_2 (produced respectively in the CH_4 and NH_3 photochemical reactions) are nearly equal. The principal reactions in the formation of CH_3NH_2 are given in Table 9. Kuhn, et al. found that at an atmospheric density level of 10^{18} cm^{-3}, nearly 60 km above the NH_3-cloud tops, the concentrations of CH_3 and NH_2 are comparable, so that the reaction R8.1 forming CH_3NH_2 becomes competitive with the others listed in Table 9. Their calculations yield maximum CH_3NH_2 production rate of 6×10^4 cm^{-3} (Jovian day)$^{-1}$, with the maximum volume mixing ratio of CH_3NH_2 of 3×10^{-11} cm^{-3} as shown in Fig. 13. Subsequent revision of the CH_4 absorption cross sections (Mount, et al. 1977) reduces the CH_3NH_2 mixing ratio by approximately 20%.

TABLE 9 PHOTOCHEMISTRY OF CH_3NH_2
(After Kuhn, Atreya and Chang, 1977)

Chemical Reactions	Reaction Number
$CH_3 + NH_2 \longrightarrow CH_3NH_2$	(R8.1)
$CH_3 + CH_3 + M \longrightarrow C_2H_6 + M$	(R8.2)
$CH_3 + H + M \longrightarrow CH_4 + M$	(R8.3)
$NH_2 + NH_2 \longrightarrow N_2H_4$	(R8.4)
$NH_2 + H + M \longrightarrow NH_3 + M$	(R8.5)

Figure 13. Volume mixing ratios of CH_3NH_2 and the related radicals in the atmosphere of Jupiter. Atmospheric number densities (cm^{-3}) corresponding to the heights are shown on the right ordinate. Reproduced from Kuhn, Atreya and Chang (1977).

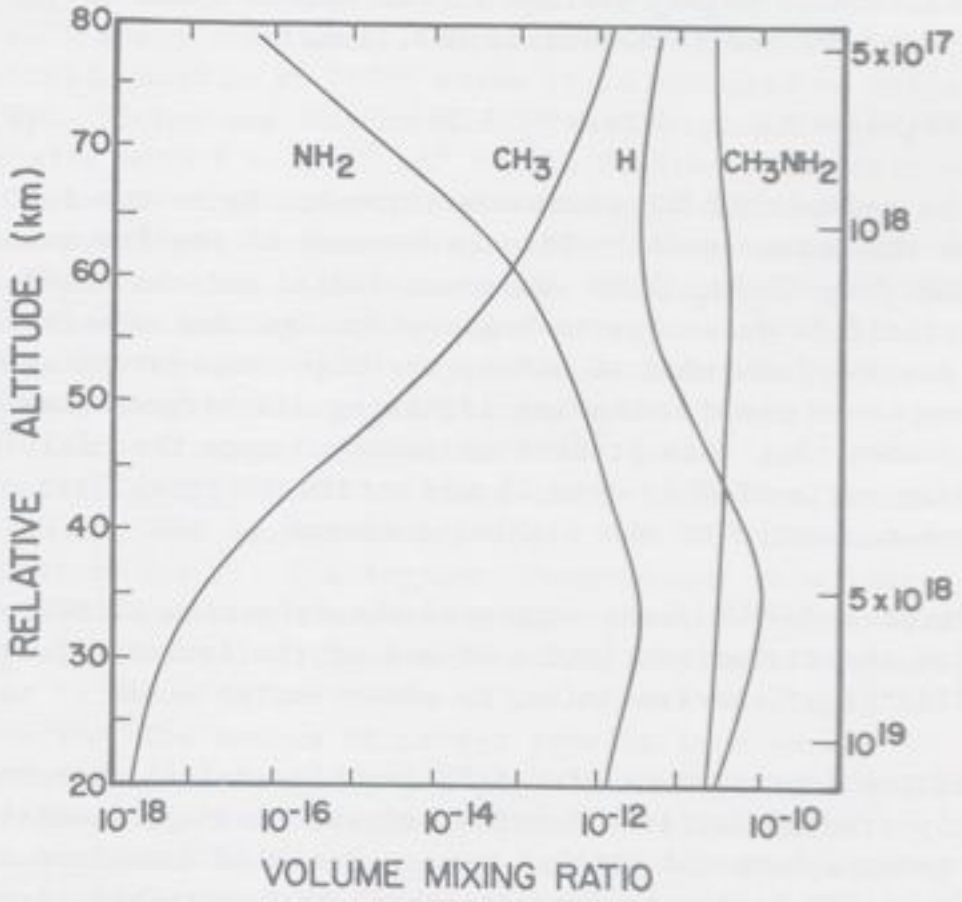

Recently, Kaye and Strobel (1983a) have followed up on a suggestion of Ferris and Chen (1975) that translationally hot hydrogen atoms produced in the photolysis of NH_3, PH_3, and C_2H_2 would react with CH_4 to produce CH_3 radicals, and subsequently result in the formation of CH_3NH_2 by reaction R8.1 in Table 9. They also included catalytic dissociation of CH_4 to (CH_3+H) as was discussed earlier (reaction R6.36). The maximum CH_3NH_2 mixing ratio obtained by Kaye and Strobel (1983a) is higher than Kuhn, et al.'s by approximately a factor of 2 which is hardly significant, considering the uncertainties in the tropospheric vertical mixing and the chemical rate constants. Furthermore, it has not been demonstrated that sufficient quantities of hot hydrogen atoms can survive thermalization at these high pressures. Methylamine has not been detected in the outer planets since its abundance is extremely low. An attempt to detect this species will be made during the descent of Galileo Probe Mass Spectrometer.

9 C-N COUPLING: HYDROGEN CYANIDE (HCN)

First definitive detection of HCN on Jupiter was made by Tokunaga, et al. (1981). They obtained column abundance of 1.3×10^{17} cm^{-2} for HCN at the tropopause. Thermochemical equilibrium cannot account for HCN in the Jovian atmosphere (Barshay and Lewis, 1978). Photodissociation of CH_3NH_2 (formed in the manner shown in Table 9) can indeed lead to the formation of HCN, i.e,.

$$CH_3NH_2 + h\nu \rightarrow HCN + H_2 + 2H \qquad (R9.1)$$

However, the calculated HCN abundance turns out to be too low compared to the measurements. This is because of the low quantum yield of HCN from CH_3NH_2 (0.08, Gardner, 1981), and the CH_3NH_2 abundance itself is quite low to begin with. Another possible mechanism for the formation of HCN is the high temperature synthesis of the atmospheric gases following lightning discharges. Lewis (1980) has shown that this process produces no more than 3×10^{-12} volume mixing ratio of HCN, even if the entire internal heat of Jupiter were converted to the lightning energy.

Kaye and Strobel (1983b) have suggested the formation of HCN on Jupiter from the photodissociation of one of the isomers of C_2H_5N, cyclic aziridine or ethyleneimine, as shown in Table 10.

Only one of the four isomers of C_2H_5N, (ethyleneimine), has been sufficiently studied for its kinetics and spectroscopy. Considering just this isomer, Kaye and Strobel have calculated a maximum of 2×10^{17} cm^{-2} of HCN at the tropopause, which is comparable to the observed abundance of this species. HCN is a precursor of amino and nucleic acids, and could therefore be important in the prebiotic atmosphere of the earth. Polymers of HCN have been proposed also as the chromophores responsible for the color of the GRS and other clouds on Jupiter (Woeller and Ponnamperuma, 1969).

TABLE 10 HCN PHOTOCHEMISTRY
(After Kaye and Strobel)

Chemical Reactions	Reaction Number
$NH_3 + h\nu \longrightarrow NH_2 + H$	(R9.2)
$H + C_2H_2 + M \longrightarrow C_2H_3 + M$	(R9.3)
$NH_2 + C_2H_3 \longrightarrow C_2H_5N$	(R9.4)
$C_2H_5N + h\nu \longrightarrow HCN + CH_3 + H$	(R9.5)

10 CARBON MONOXIDE (CO)

Beer (1975), Beer and Taylor 1978) and Larson, et al. (1978) have detected CO in the atmosphere of Jupiter. Beer and Taylor give a CO column abundance of $4.3(+4.3, -2.2)\times10^{17}$ cm^{-2}, volume mixing ratio 10^{-9}, and a rotational temperature of 125±25K. Larson, et al. (1978), on the other hand, imply a column abundance of 8×10^{17} cm^{-2} and a rotational temperature of 150-300K. CO is thermochemically stable at 1100K where it is produced on oxidation of CH_4 by H_2O. Prinn and Barshay (1977) have argued for a strong vertical mixing with $K \simeq 2\times10^{8}$ cm^2 s^{-1} in Jupiter's interior to transport CO to the upper atmosphere. The wide discrepancy in the rotational temperature of the abovementioned observations of CO allows for the source to be either in the interior of the planet, or extraplanetary. An extraplanetary source proposed by Strobel and Yung (1979) involves removal of oxygen atoms from the Galilean satellites on impact by energetic charged particles. They calculate the largest flux of oxygen at Jupiter (10^6 to 10^7 cm^{-2} s^{-1}) from Io. Lanzerotti, et al (1978) estimate the O-fluxes at Jupiter from Europa, Callisto, and Ganymede varying between 10^4 (Ganymede) to 2×10^7 (Europa) cm^{-2} s^{-1}. The Voyager observations show that although Strobel and Yung's mechanism for removing oxygen from Io is not operative, the total flux of oxygen from all Galilean satellites into Jupiter is found to be on the order of $(0.3 \text{ to } 5)\times10^7$ cm^{-2} s^{-1} (Science, 1979). The source of oxygen from Io lies in the photodissociation and charged particle dissociation of SO_2 (Kumar and Hunten, 1982) which is released from the volcanoes of Io (Morabito, et al., 1979; Hanel, et al., 1979). Subsequent ionization of oxygen leads to oxygen ions, as is evident from their large concentrations in the Io torus (Broadfoot, et al., 1979; Bridge, et al., 1979). Energetic oxygen atoms/ions entering Jupiter lose their energy in collisions with H_2. Subsequent reactions leading to the formation of CO are given in Table 11.

TABLE 11 CO PHOTOCHEMISTRY

Chemical Reactions	Reaction Number
$O + CH_3 \rightarrow HCHO + H$	(R10.1)
$HCHO + O \rightarrow HCO + OH$	(R10.2)
$HCO + O \rightarrow OH + CO$	(R10.3)
$\rightarrow H + CO_2$	(R10.4)
$HCO + H \rightarrow H_2 + CO$	(R10.5)
$O + CH_2 \rightarrow H_2 + CO$	(R10.6)

The thermal oxygen atoms react with the methyl radicals formed in the CH_4 photochemistry, and produce formaldehyde, HCHO. After a series of further chemical reactions, CO and CO_2 are produced.

In addition to the radial diffusion of oxygen from the Galilean satellites to Jupiter (Strobel and Yung, (1979), oxygen ions can also enter Jupiter along the magnetic flux tubes connecting Io to Jupiter, as was suggested for the transport of the sodium ions from Io to Jupiter by Atreya, et al. (1974).

Prather, et al. (1978) have suggested another extraplanetary source of oxygen, involving ablation of carbonaceous chondritic meteorites in the Jovian atmosphere. They estimate the flux of H_2O released to be on the order of 10^7 to 2×10^9 cm^{-2} s^{-1}. Photolysis of water produces oxygen atoms which undergo the chemical reactions given in Table 11, and eventually result in the formation of CO. Sputtering of water ice on Saturn's E-ring, and the moons Dione and Tethys can provide from 3×10^{22} to 4×10^{24} s^{-1} oxygen ions following dissociation/ionization of the water (Cheng, et al., 1982). A fraction of the oxygen atoms so produced will surely end up in Saturn's upper atmosphere and undergo chemical reactions such as those in Table 11 to produce CO.

All of the abovementioned sources provide sufficient flux of oxygen atoms (4×10^7 cm^{-2} s^{-1}) to explain the CO mixing ratio of 10^{-9} observed at Jupiter. To discriminate between them would require correct identification of the temperature-pressure regime of the origin of CO; detection of oxygen and water in the upper atmosphere of Jupiter, and its relationship to the extraplanetary source of O or H_2O.

11 CLOUD FORMATION

By assuming hydrostatic and thermodynamic equilibrium it is possible to predict the locations and densities of clouds in a planetary atmosphere. On a Jovian planet, the resulting predicted cloud structure is a multilayered one consisting of one or more of the following clouds: aqueous ammonia (in varying concentrations), water ice, solid ammonium hydrosulfide, ammonia ice, or methane ice. On Uranus, possibility exists also of the formation of acetylene and ethane clouds. So far, the most extensive application of this method of modeling the cloud structure of the Jovian planets has been done by Weidenschilling and Lewis (1973).

It is reasonable to assume that in the region of cloud formation the thermal structure of the planet is governed by a wet adiabat. An expression for the wet adiabat applicable to the Jovian planets, and subsequent formulation of the cloud densities will be discussed in the following sections.

12 DERIVATION OF THE WET ADIABATIC LAPSE RATE

Starting with the the law of energy conservation for an adiabatic expansion of one mole of a gas,

$$\bar{C}pdT - vdP + \sum_k L_k dX_k + L_{RX} dX_{H_2S} = 0 \qquad (12.1)$$

where $\bar{C}p$ is the mean molar heat capacity at constant pressure, dT is the differential change in absolute temperature, v is the molar volume, dP is the differential change in total pressure, L_k is the molar enthalpy of condensation of the k_{th} gas, dX_k is the differential change in the number of moles of the k_{th} gas due to condensation, L_{RX} is the molar heat of reaction for:

$$NH_3(g) + H_2S(g) \rightarrow NH_4SH(s) \qquad (12.2)$$

(a cold trap for NH_3 and H_2S), and dX_{H_2S} is the differential change in the number of moles of H_2S due to the reaction in equation (12.2). Since in the above reaction for every mole of hydrogen sulfide one mole of ammonia is removed the choice of dX_{H_2S} in (12.1) is arbitrary, i.e. dX_{NH_3} could have been used in place of dX_{H_2S}. The goal is to express (12.1) completely in terms of dT and dZ, the height increment.

Working first on the term -vdP, one has from hydrostatic equilibrium:

$$\frac{\bar{R}\bar{T}dP}{P} = -\bar{m}gdZ \qquad (12.3)$$

where $\bar{m}$ is the mean molecular weight of the atmosphere, g is the local acceleration due to gravity, R is the gas constant, and $\bar{T}$ is the average temperature over the height increment. From the equation of state for one mole of an ideal gas, one has

$$v = \frac{RT}{P} \qquad (12.4)$$

Substituting (12.4) into the left hand side of (12.3), one obtains

$$vdP = -\bar{m}gdZ \tag{12.5}$$

Now working on the term $\sum_k L_k dX_k$, for an ideal gas mixture:

$$X_k = P_k / P \tag{12.6}$$

where P_k is the partial pressure of the k_{th} gas . Differentiation of equation (12.6) yields

$$dX_k = dP_k / P - (P_k dP / P^2) \tag{12.7}$$

From the Clausius - Clapeyron equation and hydrostatic equilibrium, one obtains respectively:

$$dP_k = P_k L_k dT / RT^2 \tag{12.8}$$

and:

$$dP = -\bar{m}Pg dZ / RT \tag{12.9}$$

Substitution of (12.8) and (12.9) into (12.7), and use of (12.6) gives

$$\sum_k L_k dX_k = \sum_k \left(\frac{L_k^2 X_k dT}{RT^2} + \frac{L_k X_k \bar{m} g dZ}{RT}\right) \tag{12.10}$$

Lastly, one needs to express dX_{H_2S} in terms of dT, and dZ. Starting from Lewis (1969)

$$\log_{10} (P_{NH_3} \cdot P_{H_2S}) = \log_{10}(K_p) = 14.82 - \frac{4705}{T} \tag{12.11}$$

where pressure is in atmospheres, temperature in degrees Kelvin, and K_p is the equilibrium constant. For ease of computation one can write (12.11) in cgs units:

$$\ell n (P_{NH_3} \cdot P_{H_2S}) = 6.467 - \frac{10,834}{T} \tag{12.12}$$

(pressure is now in dynes / cm^2). Differentiation of (12.12) gives

$$\frac{d[P_{NH_3} \cdot P_{H_2S}]}{P_{NH_3} \cdot P_{H_2S}} = \frac{10,834 dT}{T^2} \tag{12.13}$$

expanding $P_{NH_3} \cdot P_{H_2S}$ as $X_{NH_3} \cdot X_{H_2S} \cdot P^2$, and noting that $dX_{H_2S} = dX_{NH_3}$, one obtains from (12.13):

$$\frac{(X_{H_2S}+X_{NH_3}) \cdot dX_{H_2S}}{(X_{H_2S} \cdot X_{NH_3})} = \frac{10,834dT}{T^2} - \frac{2dP}{P} \qquad (12.14)$$

Using the hydrostatic equilibrium for dP, one obtains finally:

$$L_{RX}dX_{H_2S} = L_{RX}\left[\frac{X_{H_2S} \cdot X_{NH_3}}{X_{H_2S}+X_{NH_3}}\right]\left[\frac{10,834dT}{T^2} + \frac{2\bar{m}gdZ}{RT}\right] \qquad (12.15)$$

Thus equation (12.1) has been expressed in terms of dT and dZ:

$$\frac{dT}{dZ} = \frac{-\bar{m}g}{\bar{C}_p} \frac{\left[1+\frac{1}{RT}\left[\sum_k L_k X_k + \frac{2(X_{H_2S} \cdot X_{NH_3})L_{RX}}{(X_{H_2S}+X_{NH_3})}\right]\right]}{\left[1+\frac{1}{\bar{C}_p T^2}\left[\sum_k \frac{L_k^2 X_k}{R} + \frac{(X_{H_2S} \cdot X_{NH_3})}{(X_{H_2S}+X_{NH_3})} \cdot L_{RX} \cdot 10,834\right]\right]} \qquad (12.16)$$

This final equation for the lapse rate is similar to the one Weidenschilling and Lewis give, but unfortunately there are many typographical errors in their paper where this equation is derived.

On the Jovian planets, one of the possible condensates is aqueous ammonia solution of variable concentrations. This requires modification of the $L_k dX_k$ term in (12.16). If the solution that condenses out is of concentration, C (in mole fraction of ammonia) then for every mole of solution, 1-C moles of H_2O condense out, or:

$$dX_{solution} = \frac{dX_{H_2O}}{1-C} \qquad (12.17)$$

Thus, the $L_k dX_k$ term in (12.16) due to the formation of a solution cloud can be expressed as

$$\frac{L_s dX_{H_2O}}{1-C} \qquad (12.18)$$

where L_s is the average heat of condensation of the solution. Even though the heat of condensation of the aqueous ammonia solution is a function of both the temperature and the concentration of the solution, Lewis (1969) showed it is permissible to adopt an average heat of condensation for the solution cloud. In the Jovian planets,

for various physical reasons, the solution cloud becomes more concentrated in ammonia as the temperature decreases. These two factors act to keep the heat of condensation approximately constant. At any rate, the heat of condensation varies by less than a factor of two.

13 CLOUD DENSITY

The density of a cloud in an atmosphere in hydrostatic equilibrium can be found in the following manner. Following Weidenschilling and Lewis, at a given level, J, in an atmosphere in hydrostatic equilibrium one has:

$$M^J = \frac{P^J}{g} \tag{13.1}$$

where M^J is the mass per unit area of the atmosphere above level J, and P^J is the pressure at level J. For a single constituent k, its mass per unit area in the atmosphere above level J is:

$$m_K^J \cdot M^J \tag{13.2}$$

where m^J_k is its weight fraction in the atmosphere. Thus the average cloud density, $\bar{D}$, in the altitude increment, dZ, between the levels I and J in the atmosphere due to species k condensing is:

$$\bar{D} = \frac{(m_K^I - m_K^J)\bar{M}}{dZ} \tag{13.3}$$

where $\bar{M}$ is the average mass per unit area in the condensing layer. Equation (13.4) can be rewritten in terms of mole fraction and pressure:

$$D = \frac{m_K(X_K^I - X_K^J)\bar{P}}{\bar{m}g dZ} \tag{13.4}$$

If more than one species is condensing to form the cloud (NH_4SH or aqueous ammonia cloud), the right hand side of (13.4) is summed over the condensing species.

14 CALCULATION OF CLOUD STRUCTURE

The cloud structure in a planetary atmosphere can now be calculated. The numerical scheme starts deep in the atmosphere,

before any condensation has taken place, with a specified composition, temperature, and pressure. The altitude is then incremented and the new temperature calculated from the dry adiabatic lapse rate, and the atmospheric pressure from hydrostatic equilibrium. The partial pressures of the condensates are then found from the atmospheric pressure and their respective mole fractions. The equilibrium vapor pressures of the condensates are computed from the temperature and empirical equations. If the partial pressure of a condensate is greater than its equilibrium vapor pressure, or for the case of ammonium hydrosulfide if its equilibrium constant is exceeded, some formation of that condensate occurs. The partial pressures of the condensing species are then set equal to their respective equilibrium vapor pressures, and their new mole fractions in the atmosphere are calculated. The altitude is incremented again and the new temperature is calculated from the appropriate wet adiabatic lapse rate using a Kutta - Simpson fourth order method, or the dry adiabatic lapse rate if nothing condensed out. This cycle is repeated until the tropopause temperature is reached.

For most of the condensates, empirical vapor pressure equations are easily found in such sources as the International Critical Tables. However, to calculate the vapor pressures of ammonia and water over aqueous ammonia solutions is a bit more complicated. The saturation vapor pressures of ammonia and water are available for the temperature range 273 - 363 K (Wilson 1925, Linke 1965, ICT 1928), but on the Jovian planets it is be possible to have solution clouds at much lower temperatures. Thus there is a need to extapolate the saturation partial pressures below the limits of available laboratory data. Starting with the Clausius - Clapeyron equation in the form:

$$\frac{dP}{dT} = \frac{\Delta HP}{RT^2} \qquad (14.1)$$

(where ΔH is the heat of transformation). Assuming ΔH to be linear with T, the integral of (14.1) yields an equation of the form:

$$\ell n(P) = A + B/T + C\ \ell n(T) \qquad (14.2)$$

where P is the saturation partial pressure of either H_2O or NH_3 vapor above aqueous ammonia at the temperature T, and A, B, and C are functions of the mole fraction of ammonia in the solution. Various forms for the equations representing the functions were

tried, but since the analysis was for eventual use in a numerical model, a routine was developed to approximate these functions by fitting piecewise cubic splines to the data points. Thus at a given temperature, the saturation partial vapor pressures of both ammonia and water are computed at a test concentration. If the atmospheric partial pressures of ammonia and water simultaneously exceed their respective saturation partial pressures over a solution of that test concentration, then condensation of that test solution occurs. If not, the test concentration is stepped until the complete range of test concentrations is checked for possible condensation.

Our handling of the solution cloud as discussed above is different from Weidenschilling and Lewis in two aspects. Rather than using the Clausius - Clapeyron method to get the saturation vapor pressures of NH_3 and H_2O, they derived an equation for each component, "The partial vapor pressure of either NH_3 or H_2O in solution at any temperature and concentration was expressed as the product of the vapor pressure of the pure liquid phase at the temperature and a fifth order polynomial in the concentration." The coefficients of the polynomial were made to agree with Henry's Law or Raoult's Law in their respective limits. We attempted an identical analysis and obtained nearly acceptable results using temperature dependent coefficients predicted by a least squares regression routine. But the variation of the coefficients with temperature was in no way regular, and "predicted" partial vapor pressures at temperatures greater than 20 degrees below the freezing point of water were completely unrealistic. We also differ in the way the concentration of the solution cloud is calculated. We determine the base of the solution cloud in the same way as Weidenschilling and Lewis, the partial pressures of both H_2O and NH_3 in the atmosphere must exceed their respective partial saturation vapor pressures of a given concentration. We continue to use that criteria for the rest of the solution cloud to determine the concentration of the cloud. Weidenschilling and Lewis, however, use a different method to compute the concentration of the solution. They start with "a closed system containing a solution of concentration C in equilibrium with a gas at temperature, T, and total pressure P" (i.e. the base of the cloud) thus the partial pressures of ammonia and water are set equal to their equilibrium vapor pressures. Then, they step up in altitude, so that the system expands adiabatically by an infinitesimal amount, some condensation occurs, which changes the concentration of the solution. This procedure enables them to develop an expression for dC, the change in concentration of the solution, and thus the new concentration. The technique we used is

numerically more straightforward, and physically realistic.

If a solution cloud does form in the atmosphere a further complication arises. Since the resulting solution is a weak base, hydrogen sulfide, a weak acid, dissolves into it. To take this into account we have used an empirical expression developed by Leyko (1964):

$$p = \exp\left(22.221 - \frac{5388}{T}\right) C_{H_2S}^{1.130} \left(\frac{C_{H_2S}}{C_{NH_3}}\right)^{1.8953} \qquad (14.3)$$

where p is the vapor pressure of H_2S in mm of Hg above the solution, T is the temperature in degrees kelvin, C_{H_2S} is the mol/liter of hydrogen sulfide in the solution, and C_{NH_3} is the mol/liter of ammonia in the solution. Taking both the molar concentration of NH_3 and the temperature as fixed, the equilibrium partial pressure of H_2S in the atmosphere is found by an iterative process.

15 RESULTS, DISCUSSION, SUGGESTIONS

Like Weidenschilling and Lewis we considered the possible condensation of aqueous ammonia, water ice, ammonium hydrosulfide, ammonia ice, methane ice, and argon ice. We do not consider, yet, the liberation of heat of conversion from para-to ortho-hydrogen as has been proposed by Gierasch (1983) and Massie and Hunten (1982). The equilibrium distribution of ortho to para H_2 is a function of temperature. The most likely mechanism to enable the equilibration and thus liberation of heat in the upper tropospheres of the Jovian planets is surface catalysis. So, this will most likely take place in dense cloud regions. This conversion also affects the C_p of H_2.

Figures 14 and 15 show the cloud structure for nominal Jupiter and Saturn cases. The cloud densities are given in Table 12. Both are for solar composition atmospheres. We used the Voyager RSS data to set the temperature at the initial pressure levels for these models. The Voyager observations actually yield temperatures in the upper troposphere (Jupiter: 150 K at 0.6 bars, Eshleman, et. al. 1979; Saturn: 143±6 K at 1.2 bars, Tyler, et. al. 1981). To get a temperature at a pressure level deep enough in the atmosphere we make use of the following relation from Banks & Kockarts (1973):

$$P = P_o \left(\frac{H}{H_o}\right)^{-1/\beta} \qquad (15.1)$$

TABLE 12

COMPARISON OF CLOUD DENSITIES ON JUPITER AND SATURN FOR A SOLAR COMPOSITION ATMOSPHERE WITH VOYAGER THERMAL PROFILES

	NH_3-H_2O Solution		H_2O Ice		NH_4SH(s)		NH_3 Ice	
	Jupiter	Saturn	Jupiter	Saturn	Jupiter	Saturn	Jupiter	Saturn
Begin Pressure (bars)	Non existent	9.94	4.25	9.00	1.76	3.71	0.506	1.07
End+	Non existent	9.18	1.45	2.99	1.19	2.45	0.299	0.629
Begin Temperature (K)	Non existent	280	268	272	207	210	143	145
End+	Non existent	274	196	197	185	185	122	124
Density at cloud base (gm cm^{-3})	Non existent	3.95×10^{-5}	1.97×10^{-5}	2.26×10^{-5}	1.45×10^{-7}	2.06×10^{-6}	5.18×10^{-7}	5.56×10^{-7}
Integrated cloud density (gm cm^{-2})	Non existent	26.24	12.08	39.88	0.4507	1.661	0.1580	0.4776

+end is defined to be when the cloud density is 10^{-5} gm/l, except for the NH_3-H_2O solution cloud where end is defined to be where it merges with the H_2O ice cloud.

Figure 14. Cloud structure of the Jovian atmosphere for a solar composition atmosphere and thermal profile from Voyager observations. The NH_4SH cloud is composed of solid particles. Altitudes are relative from a base level of T = 425 K at P = 200 bars. Cloud densities are log base 10, g = 2325 cm sec $^{-2}$, and the average lapse rate is 1.9 K km $^{-1}$.

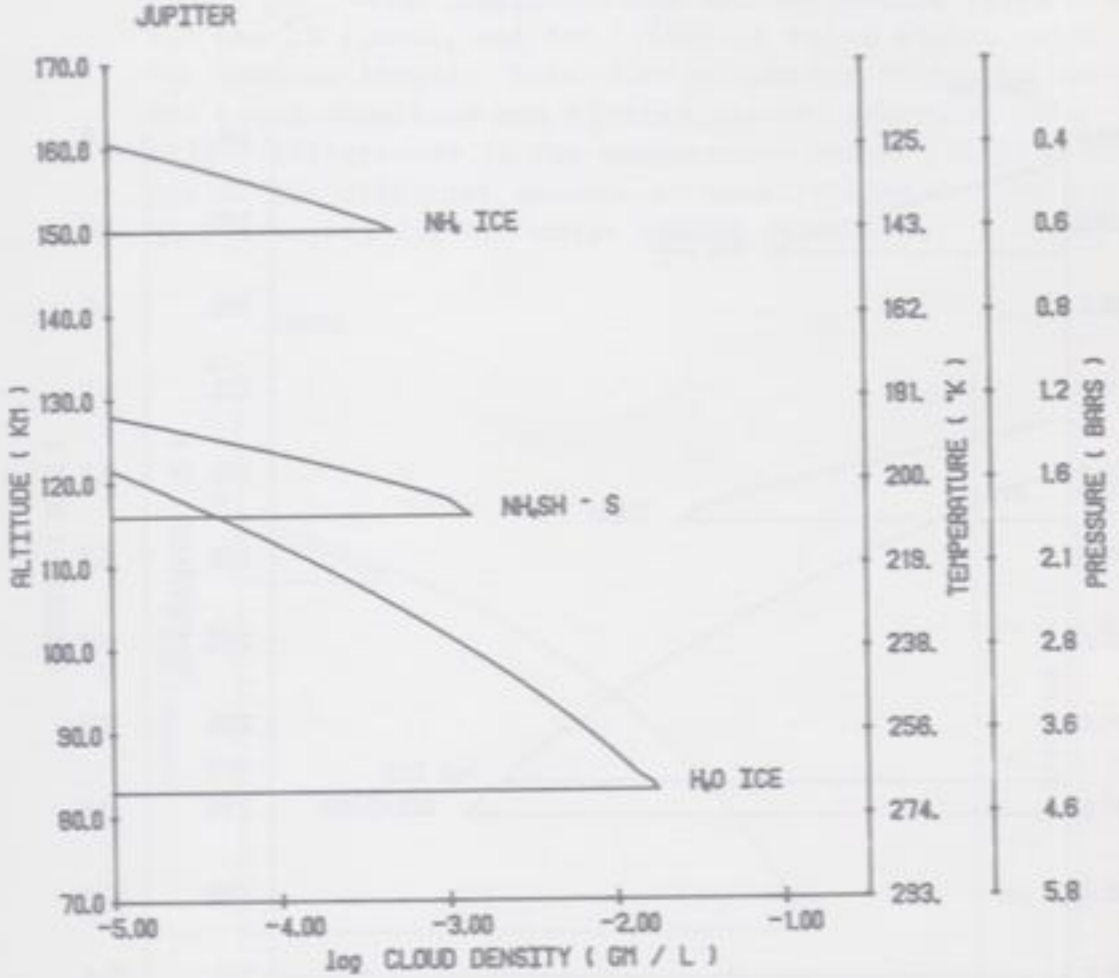

where P_o and H_o are the pressure and atmospheric scale height respectively in the upper troposphere (known values), P is the pressure at some level deep in the atmosphere before any condensation has taken place, H is the scale height at that deep level, and β is the derivative of the scale height with respect to altitude. For an initial approximation we assume that the change in scale height with altitude is due to the dry adiabatic lapse rate or:

$$\beta = \frac{\bar{k}}{\bar{m}g}\frac{dT}{dZ} = \frac{-\bar{k}}{\bar{m}g}\frac{g}{\bar{c}_p} = \frac{-\bar{k}}{\bar{m}\bar{c}_p} \text{(where } \bar{c}_p \text{ is in erg gm}^{-1}\text{ K}^{-1}\text{)} \quad (15.2)$$

Figure 15. Cloud structure of the Saturnian atmosphere for a solar composition atmosphere and thermal profile from Voyager observations. The NH_4SH cloud is composed of solid particles. Altitudes are relative from a base level of T = 400 K at P = 330 bars, cloud densities are log base 10, g = 1000 cm sec $^{-2}$, and the average lapse rate is 0.81K km $^{-1}$. The aqueous ammonia solution cloud is a thin layer just below the H_2O-ice cloud.

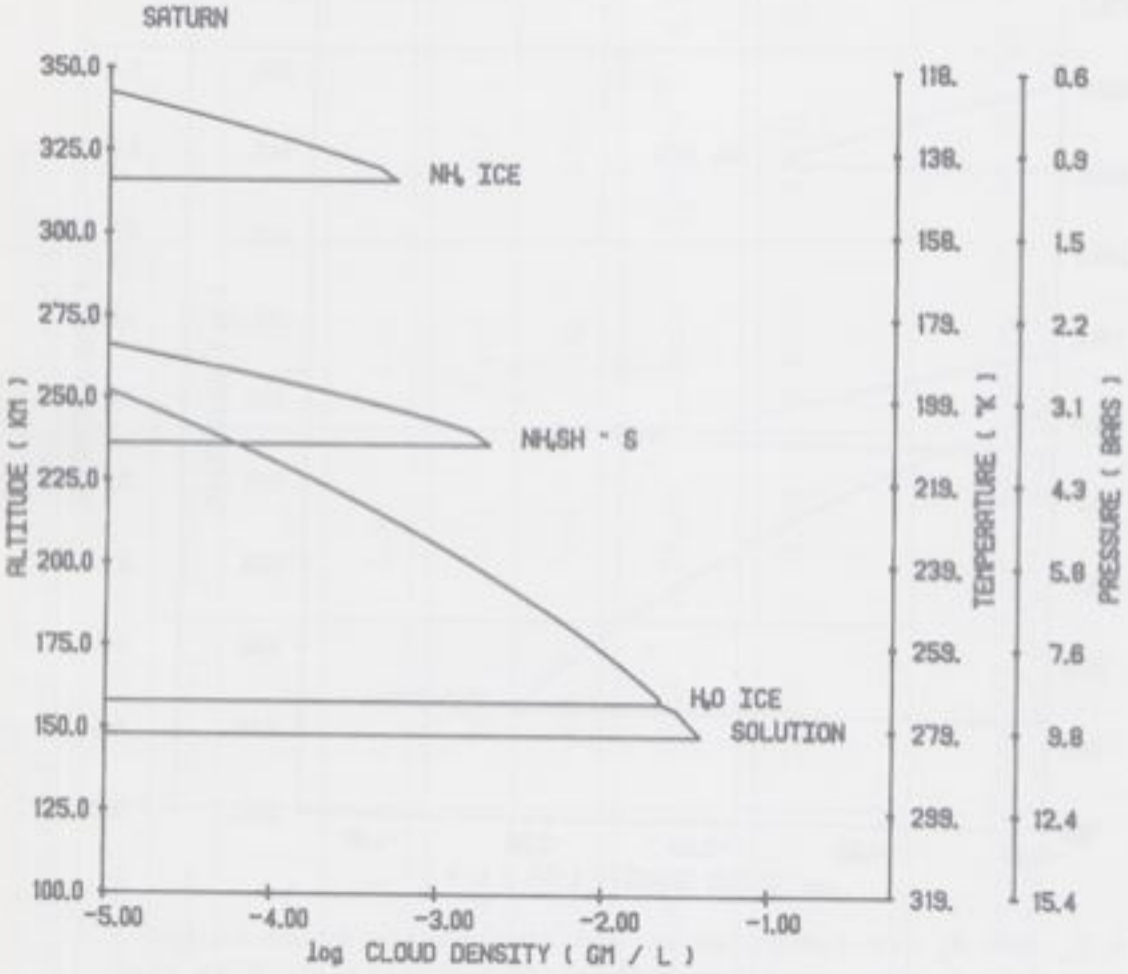

A high temperature is picked deep enough in the atmosphere where condensation has not yet taken place, thus fixing the value of the scale height. Using equations (15.1) and (15.2), the pressure is determined at that level taking into account the additional heat liberated in the atmosphere due to condensation.

There has been one ground-based observation of water on Jupiter (Larson, et al., 1975), and one observation from Voyager/IRIS

(Kunde, et al., 1982), both in the belt region. These measurements yield the H_2O mixing ratio to be approximately 1/1000 of the solar value. These measurements should not be construed to represent the global average of water on Jupiter. If dry spots do exist on Jupiter, only a thin, low density water ice cloud would be expected as is apparent from the calculations shown in Fig. 16.

Figure 16. Water ice cloud for a solar mixing ratio of H_2O (solid lines), and for 1/1000 of solar mixing ratio of H_2O (dashed lines). Note that to compare these two cases the cloud densities are plotted against pressure. The slight differences in the temperature-height profiles are due to the different amounts of heat liberated. The left hand axes are for the solar mixing ratio case.

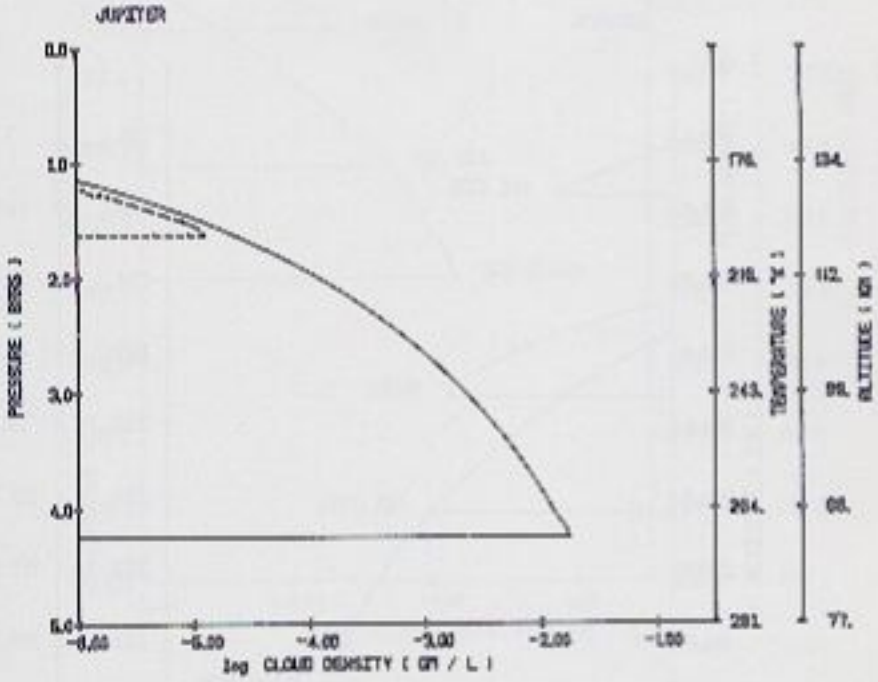

As less is known about Uranus, compared to Jupiter and Saturn, we have had to parametrize several quantities in our Uranus cases. Figures 17, 18, and 19 represent respectively a "cold" solar composition Uranus, a "warm" solar composition Uranus, and lastly a "cold" Uranus with NH_3, H_2O, CH_4, and H_2S in ten times solar amounts. Since Uranus does not appear to possess an internal heat source, its temperature in the interior is expected to become

isothermal at some pressure. (Note that the cold case used here is still a lot warmer than the cold thermal model of Palluconi (1972) used by Gulkis, et al. (1978) to explain their NH_3 data as discussed later). Furthermore, as discussed in Sec. 2, there is a likelihood of higher than solar mixing ratios of NH_3, H_2S, H_2O, etc., on Uranus. In view of the above, we feel that the 'cold' case with 10 x solar NH_3, H_2O, and H_2S is more representative of the temperature and composition of the deep troposphere of Uranus.

Figure 17. Cloud structure of "cold" (T = 450 K at P = 670 bars base level), solar composition Uranus. The NH_4SH cloud is composed of solid particles. Altitudes are relative from the base level, cloud densities are log base 10, g = 900 cm sec^{-2}, and the average lapse rate is 0.72 K km^{-1}.

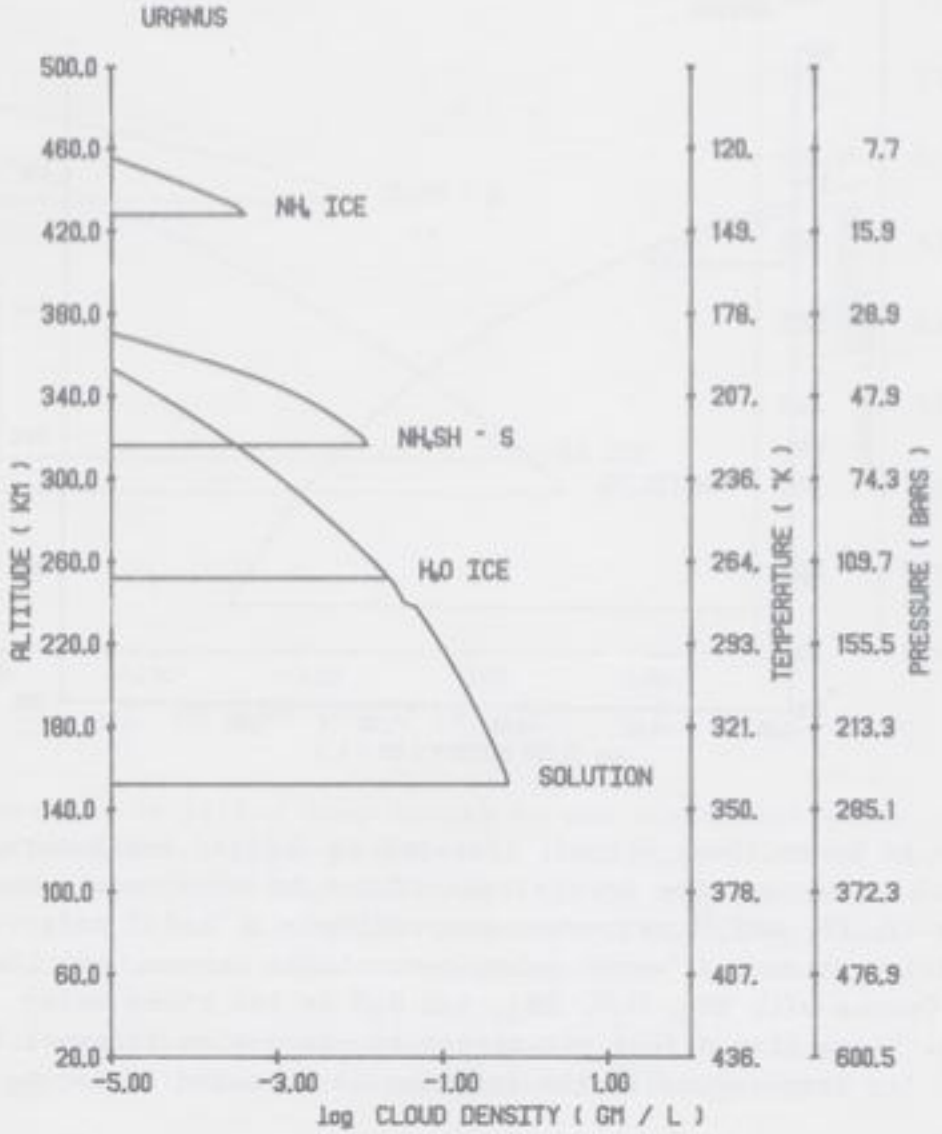

Figure 18. Cloud structure of "warm" (T = 450 K at P = 250 bars base level) solar composition Uranus. The other parameters are same as in Figure 17.

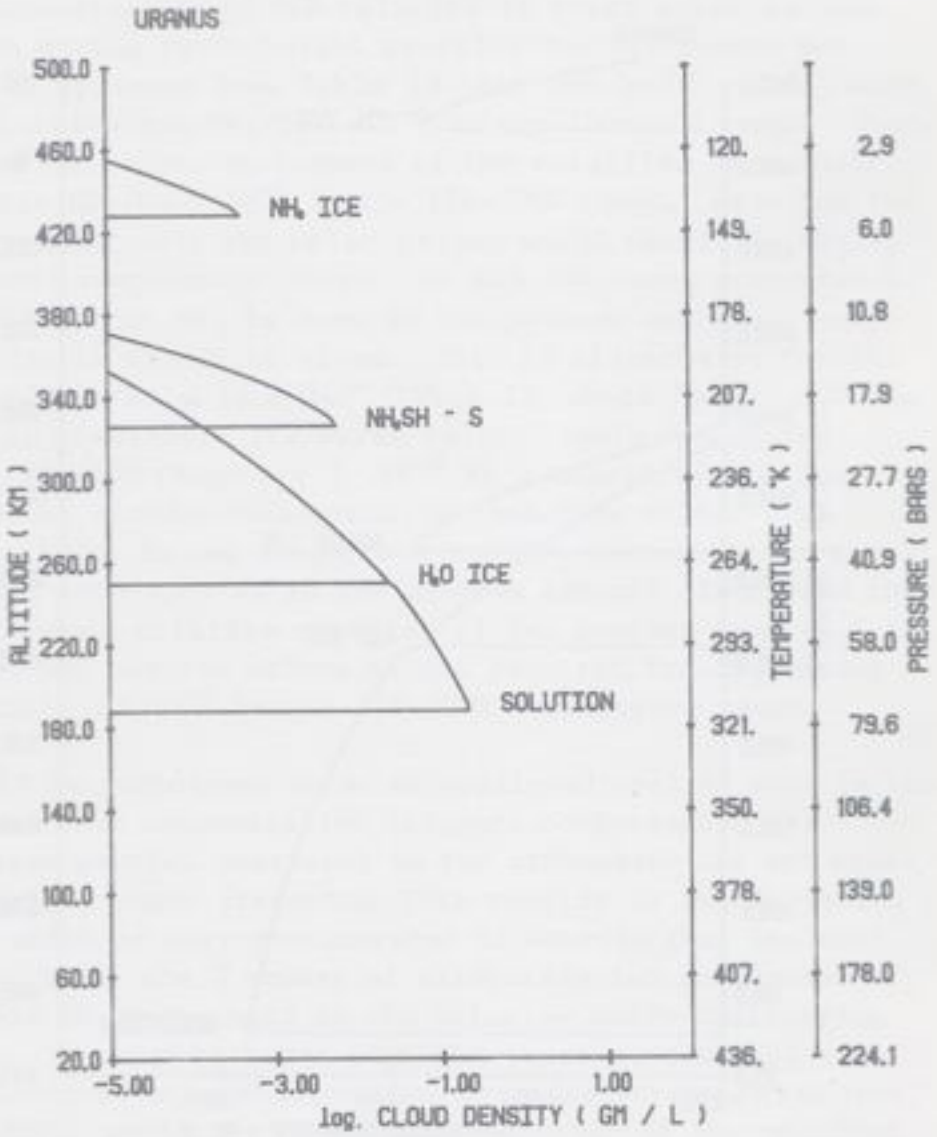

Figure 19. Cloud structure of "cold" Uranus with NH_3, H_2O, CH_4, and H_2S in ten times solar amounts. The other parameters are same as in Figure 17.

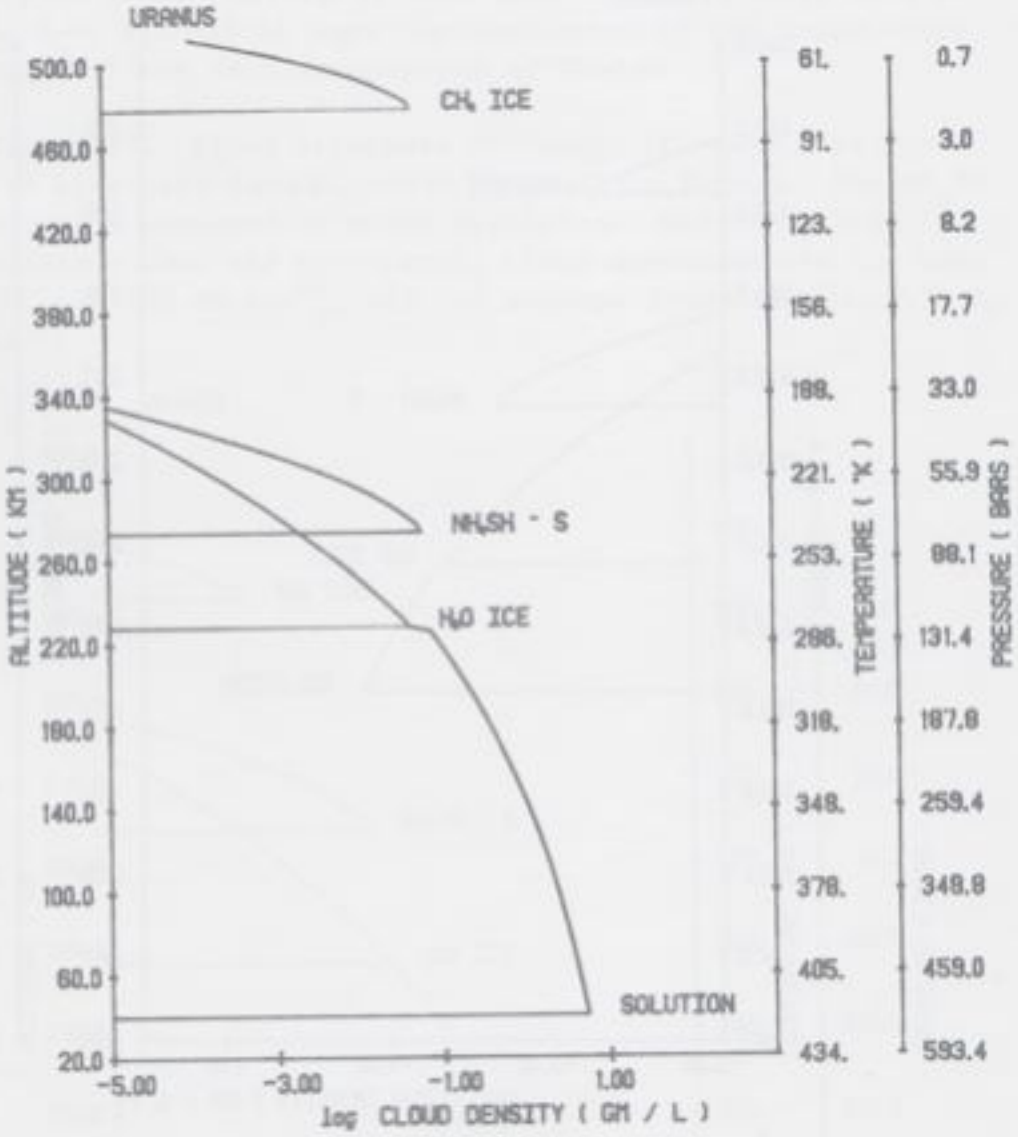

Gulkis, et al. (1978) have made microwave observations of Uranus. They discovered that the NH_3 mixing ratio in the atmosphere of Uranus in the temperature range 150K - 200K must be less than 10^{-6}, i.e., much below solar. They propose that H_2S is enriched preferentially (and not NH_3) above its solar mixing ratio, so that

the NH_4SH cold trap reaction depletes NH_3 completely. (In a solar composition atmosphere the ammonia mixing ratio is about ten times that of hydrogen sulfide, so the ammonium hydrosulfide cloud will always leave excess ammonia). We feel a more plausible mechanism for the depletion is loss of NH_3 in the aqueous ammonia cloud. This does not require increasing S/N or O/N relative to their solar values. For the ammonia mixing ratio height profiles for our cases, see Table 13. It is apparent from Table 13 that the 'cold' case with 10 x solar volatiles has $NH_3/H_2 << 10^{-6}$ in the 150-200K range. Thus, one requires only a slight enrichment of the volatiles over their solar values for $NH_3/H_2 \leq 10^{-6}$ in the 150-200K range. Even for the warm case, enrichment over the solar values would result in $NH_3/H_2 < 10^{-6}$ in the above temperature range. In all the cases presented in Table 13, 70-90% of the NH_3 is lost in the aqueous ammonia cloud, and the remaining in the NH_4SH cloud. This is illustrated further in the case labeled 'cold 10 x H_2O' (Table 13) where 'only' H_2O has been enriched 10 times over its solar value. Again NH_3 mixing ratios in the 150-200K range are $\leq 10^{-6}$ as a result of the loss of NH_3 in the aqueous cloud. These results therefore differ from Gulkis, et al. (1978) in two respects: low NH_3 mixing ratios result from the loss of this species in the aqueous ammonia cloud, and that selective enrichment relative to solar of one species (e.g., H_2S in Gulkis, et al.) and not the others is not required for NH_3 mixing ratio to remain below 10^{-6} in the 150-200K temperature range.

A caveat should be introduced here. As mentioned earlier when in the solution cloud a test concentration triggers condensation the ammonia and water partial pressures in the atmosphere are set equal to their saturation vapor pressures. This results in the formation of a solution which is more concentrated in ammonia than the test concentration. There are a number of disequilibrium mechanisms which may enable NH_3 to be held in the solution above equilibrium concentrations. It is well known that the vapor pressure of a substance is lower over a solution than over the pure solvent (see, e.g., Mason, 1957), and it is reduced even further if the solution is a multi-component one, or it is 'doped' with impurities. The behavior of a highly polar molecules such as water is even more complicated, particularly in the presence of a less polar molecule such as NH_3. The fugacity of water over aqueous solutions of electrolytes is reduced below the value over non-electrolyte solutions of the same molar concentration. Under similar conditions, the fugacity of ammonia is not expected to be reduced as much. The laboratory measurements we have of the equilibrium vapor pressures are of only ammonia and water above the aqueous solution,

TABLE 13
AMMONIA MIXING RATIOS ON URANUS

T	COLD			WARM	
	Solar	10 x Solar	10 x H_2O	Solar	10 x Solar
125	1.2×10^{-7}	0	0	3.3×10^{-7}	1.4×10^{-7}
150	4.0×10^{-6}	0	0	9.2×10^{-6}	1.4×10^{-7}
175	4.0×10^{-6}	3.6×10^{-11}	1.0×10^{-10}	9.2×10^{-6}	2.0×10^{-6}
200	4.2×10^{-6}	3.2×10^{-8}	9.4×10^{-8}	1.0×10^{-5}	3.0×10^{-5}
225	1.5×10^{-5}	6.2×10^{-6}	8.9×10^{-7}	2.2×10^{-5}	4.4×10^{-5}

Notes COLD model has T = 450K at P = 670 bars
WARM model has T = 450K at P = 250 bars

'Solar' case has O/H, C/H, N/H and S/H in the solar ratios of the elements.

'10 x Solar' case has O/H, C/H, N/H and S/H in 10 x Solar ratios of the elements.

'10 x H_2O' case has only O/H = 10 x Solar; C/H, N/H and S/H are in the solar ratios.

not over a fluid mixture. It is conceivable that He, an inert gas, and H_2, a homonuclear molecule, may have no effect on the vapor pressures beyond that to make an external pressure correction to the vapor pressures. But in a solar composition atmosphere there is 5 times as much methane as there is ammonia. Other species such as phosphine, germane, etc., can form oxides by dissolving in water. All this may have a significant effect on the equilibrium vapor pressures. What is really needed to shed light on these topics is good laboratory measurements of the equilibrium vapor pressures of aqueous ammonia over a solar composition mixture of fluids in the temperature and pressure ranges of interest to the outer planets.

The Uranus cloud structures shown in Figs. 17, 18 and 19 extend to an altitude just below the tropopause. However, condensation of the hydrocarbons not shown in these figures is a distinct possibility near and above the tropopause of Uranus. As seen earlier (Sec. 6) the methane photochemistry at Uranus produces C_2H_4, C_2H_2 and C_2H_6 as the principal stable hydrocarbons (Fig. 11 and 12). Subsequent production of the heavier hydrocarbons propane, butane, methylacetylene, etc. is probable, but less likely, than on Jupiter and Saturn. At the inversion layer (100mb) or the tropopause, the calculated CH_4 mixing ratio for the nominal case is 2.4×10^{-4} (see Sec. 2), whereas the value proposed by Wallace (1980) for the deep troposphere lies between 10^{-1} and 10^{-2}. Thus, condensation of CH_4 in the vicinity of the inversion layer is likely. Even if CH_4 abundance was close to solar as proposed by Teifel (1983), i.e., $CH_4/H_2 = 7 \times 10^{-4}$, one could still expect some condensation of CH_4. The calculated partial pressure of C_2H_2 is 10^8 times greater than the saturation vapor pressure at the inversion level (see Figs. 11 and 12). This implies that C_2H_2 would definitely condense and snow-out on Uranus. C_2H_2 has not been detected either on Uranus or Neptune. For C_2H_6, the ratio between the calculated partial pressure and the saturation vapor pressure at the inversion layer (55K, 100mb) is 10^2, which raises a distinct possibility of C_2H_6 condensation and subsequent snow-out, if sufficient condensation nuclei were available. C_2H_6 has not been detected on Uranus, but has been seen on Neptune which has a warmer inversion layer. The methane photolysis calculations for Uranus thus suggest that CH_4, C_2H_2, and C_2H_6 are likely to form an extended haze on Uranus. C_2H_4 abundances are too low for condensation. In the high latitudes, the extent of the haze is reduced, as is implied by curve e, Fig. 11. This can give rise to a brighter polar region as the North-pole begins to point toward the Sun. By the same reasoning, one would expect that on Neptune the clouds and hazes would be more extensive

in the polar than the equatorial regions. For the most part, the haze would be of C_2H_2 (and some C_2H_6) on both planets.

In addition to the above mentioned laboratory measurements, a better understanding of the NH_4SH reaction (kinetics and equilibrium constant), and measurements of the vapor pressures of the condensates above their respective ices in the presence of a solar composition gas in the temperature range of interest would help the modeling of the Jovian cloud structure immensely. An important next step in the cloud modeling is inclusion of irreversible pseudo-adiabatic processes in which the condensate falls out of the cloud.

SUMMARY

Photochemistries of NH_3 and CH_4 on Jupiter and Saturn are fairly well understood. This cannot be said for PH_3 or CO, which require additional laboratory measurements as well as in-situ data to discriminate between the planetary and extraplanetary origins of these species. Phosphine, elemental sulfur, hydrogen polysulfides and polymers of HCN are likely candidates for the chromophore of the Great Red Spot and other brown clouds of Jupiter. Thermochemicial equilibrium calculations for Jupiter, Saturn and Uranus predict clouds of ammonia, ammonium hydrosulfide and aqueous ammonia. The ammonia cloud on Uranus is thin to non-existent, it is, however, expected to have clouds and hazes of CH_4, C_2H_2 and C_2H_6, in addition to clouds of H_2O ice and aqueous ammonia. Little is known about possible disequilibrating processes which could alter the cloud densities calculated from thermodynamical equilibrium considerations. Improved laboratory data on the vapor pressures over impure aqueous solutions is needed to resolve important questions concerning loss of ammonia on Uranus.

ACKNOWLEDGMENT

We thank M. Wolfson for initially setting up the cloud physics code. We have benefited from discussion with T. C. Owen, S. Gulkis, and I. dePater. This work was supported by a grant from the Planetary Atmospheres Program of NASA Earth and Solar System Exploration Division.

REFERENCES

Ackerman, M. (1971) Ultraviolet solar radiation related to mesospheric processes. In Mesospheric Models and Related Experiments, ed. G. Fiocco, p 149. Dordrecht, Holland: Reidel.

Atreya, S.K. (1982) Eddy diffusion coefficient on Saturn. Planetary & Space Sci., 30, 849-854.

Atreya, S.K. & Donahue, T.M. (1979) Models of the Jovian upper atmosphere. Rev. Geophys. Space Phys., 17, 388-396.

Atreya, S.K., Donahue, T.M. & Festou, M.C. (1981) Jupiter: structure and composition of the upper atmosphere. Astrophys. J. Lett., 247, L43-L47.

Atreya, S.K., Donahue, T.M. & Kuhn, W.R. (1977) The distribution of ammonia and its photochemical products on Jupiter. Icarus, 31, 348-355.

Atreya, S.K., Donahue, T.M. & Kuhn, W.R. (1978) Evolution of a nitrogen atmosphere on Titan. Science, 201, 611-614.

Atreya, S.K., Kuhn, W.R. & Donahue, T.M. (1980) Saturn: tropospheric ammonia and nitrogen. Geophys. Res. Lett., 7, 474-478.

Atreya, S.K., Donahue, T.M. & McElroy, M.B. (1974) Jupiter's ionosphere: prospects for Pioneer 10. Science 184, 154.

Atreya, S.K. & Ponthieu (1983) Photolysis of methane and the ionosphere of Uranus. Planet. Space Sci., to be published.

Atreya, S.K. & Waite, J.H., Donahue, T.M., Nagy, A.F., & McConnell, J.C. (1984) A chapter In Saturn, ed. T. Gehrels. Tucson: University of Arizona Press.

Banks, P.M. & Kockarts, G. (1973) Aeronomy, Part A, Chapter 3. New York: Academic Press.

Barshay, S, & Lewis, J.S. (1978) A chemical structure of the deep atmosphere of Jupiter. Icarus, 33, 593-611.

Beer, R. (1975) Detection of carbon monoxide on Jupiter. Astrophys. J., 200, L167-L170.

Beer, R. & Taylor, F.W. (1978) The abundance of carbon monoxide in Jupiter. Astrophys. J., 221, 1100.

Beer, R. & Taylor, F.W. (1979) Phosphine absorption in the sun window of Jupiter. Icarus, 40, 189.

Bosco, S.R., Brobst, W.D., Nova, D.F. & Stief, L.J. (1983) The reaction $NH_2 + PH_3$ $NH_3 + PH_2$: absolute rate constant measurement and implication for $NH_3 + PH_3$ photochemistry in the atmosphere of Jupiter. J. Geophys Res., submitted.

Bridge, H.S., Belcher, J.W., Lazarus, A.J., Sullivan, J.D., McNutt,

R.L., Bagenal, F., Scudder, J.D., Sittler, E.C., Siscoe, G.L., Vasyliunas, V.M., Goertz, C.K. & Yeates, C.M. (1979) Plasma observations near Jupiter: initial results from Voyager 1, Science 204., 987.

Broadfoot, A.L., Belton, M.J.S., Takacs, P.Z., Sandel, B.R., Shemansky, D.E., Holberg, J.B., Ajello, J.M., Atreya, S.K., Donahue, T.M., Moos, H.W., Bertaux, J.L., Blamont, J.E., Strobel, D.F., McConnell, J.C., Dalgarno A., Goody, R. & McElroy, M.B. (1979) Extreme ultraviolet observations from Voyager 1 encounter with Jupiter. Science, 204, 979-982.

Cheng, A.F., Lanzerotti, L.J. & Pirronello, V. (1982) Charged particle sputtering of ice surfaces in Saturn's magnetosphere. J. Geophys. Res. 87, 4567-4570.

Clarke, J.T. (1982) Detection of auroral H Ly emission from Uranus. Astrophys. J. Lett., 263, 405.

Clarke, J.T. & Atreya, S.K. (1983) Continued studies of the bright Lyman-Alpha emission from Uranus. In preparation.

Courtin, R., Gautier, D. & Lacombe, A. (1978) On the thermal structure of Uranus from infrared measurements. Astron. & Astrophys. 63, 97-101.

Eshleman, V.R., Tyler, G.L., Wood, G.E., Lindal, G.F., Anderson, J.D., Levy, G.S. & Croft, T.A. (1979) Radio science with Voyager 1 at Jupiter: preliminary profiles of the atmosphere and ionosphere. Science, 204, 976-978.

Ferris, J.P. & Benson, R. (1980) Diphosphine is an intermediate in the photolysis of phosphine to phosphorus and hydrogen. Nature, 285, 156-157.

Ferris, J.P. & Chen, C.T. (1975) Photosynthesis of organic compounds in the atmosphere of Jupiter. Nature, 258, 587-588.

Festou, M.C. & Atreya, S.K. (1982) Voyager ultraviolet stellar occultation measurements of the composition and thermal profiles of the Saturnian upper atmosphere. Geophys. Res. Lett., submitted.

Festou, M.C., Atreya, S.K., Donahue, T.M., Shemansky, D.E., Sandel, B.R. & Broadfoot, A.L. (1981) Composition and thermal profiles of the Jovian upper atmosphere determined by the Voyager ultraviolet stellar occultation experiment. J. Geophys. Res., 86, 5715-5725.

Fowles, P., deSorgo, M., Yarwood, A.J., Strauss & Gunning, H.E. (1967) The reactions of sulfur atoms. IX. The flash photolysis of carbonyl sulfide and the reactions of S(¹D) atoms with hydrogen and methane. J. Am. Chem. Soc., 89, 1352-1359.

French, R.G., Elliot, J.L., Dunham, E. W., Allen, D.A., Elias, J.H., Frogel, J.A. & Liller, W. (1983) The thermal structure and energy balance of the Uranian upper atmosphere. Icarus, 53, 399-414.

Gardner, E.P. (1981) The vacuum ultraviolet photolysis of methylamine with application to the outer planets and Titan. Ph.D. Thesis, University of Maryland.

Gautier, D., Bezard, B., Marten, A., Baluteau, J.P., Scott, N., Chedin, A., Kunde, V. & Hanel, R. (1982) The C/H ratio in Jupiter from the Voyager infrared investigation. Astrophys. J., 257, 901-912.

Gierasch, P.J. (1983) Dynamical consequences of orthohydrogen-parahydrogen disequilibrium on Jupiter and Saturn. Science, 219 847-849.

Gladstone, G.R. (1982) Radiative transfer and photochemistry in the upper atmosphere of Jupiter. Ph.D. Dissertation, California Institute of Technology.

Gulkis, S, Jansen, M.H. & Olsen, T.E. (1978) Evidence for the depletion of ammonia in the Uranus atmosphere. Icarus, 34, 10-19.

Hanel, R.A., Conrath, B., Flaser, M., Kunde, V., Lowman, P., Maguire, W., Pearl, J., Pirraglia, J., Samuelson, R., Gautier, D., Gierasch, P., Kumar, S. & Ponnamperuma, C. (1979) Infrared observations of the Jovian system from Voyager 1. Science, 204, 972-976.

Hanel, R., Conrath, B., Flaser, F.M., Kunde, V., Maguire W, Pearl, J., Pirraglia, J., Samuelson, R., Herath, L., Allison, M., Cruikshank, D., Gautier, D., Gierasch, P., Horn, L., Koppany, R. & Ponnamperuma, C. (1981) Infrared observations of the Saturnian system from Voyager 1. Science, 212, 192-200.

Hinteregger, H.E. (1981) Representations of solar EUV fluxes for aeronomical applications. Adv. Space Res., 1, 39-52.

Hunten, D.M. (1975) Vertical transport in atmospheres. In Atmosphere of Earth and Planets, ed. B.M. McCormac, pp. 59-72. Dordrecht, Netherlands: D. Reidel.

Ingersoll, A.P., Orton, G.S., Munch, G., Neugebauer, G. & Chase, S.C. (1980) Pioneer Saturn infrared radiometer: preliminary results. Science, 207, 439-443.

International Critical Tables (1928) New York: McGraw-Hill Book Co., Inc.

Kaye, J.A. & Strobel, D.F. (1983a) Formation and photochemistry of methylamine in Jupiter's atmosphere. Icarus, in press.

Kaye, J.A. & Strobel, D.F. (1983b) HCN formation on Jupiter. The

coupled photochemistry of ammonia and acetylene. Icarus, in press.

Kuhn, W.R., Atreya, S.K. & Chang, S. (1977) The distribution of methylamine in the Jovian atmosphere. Geophys. Res. Lett., 4, 203-206.

Kumar, S. & Hunten, D.M. (1982) The atmosphere of Io and other satellites. In The Satellites of Jupiter, ed. D. Morrison, pp. 782-806. Tucson: University of Arizona Press.

Kunde, V., Hanel, R., Maguire, W., Gautier, D., Baluteau, J.P., Marten, A., Chedin, A., Husson, N. & Scott, M. (1982) The tropospheric gas composition of Jupiter's north equatorial belt (NH_3, PH_3, CH_3, GeH_4, H_2O) and the Jovian D/H isotopic ratio. Astrophys. J., 263, 443-467.

Lanzerotii, L.J., Brown, W.L., Poate, J.M. & Augustyniak, W.M. (1978) On the contribution of water products from Galilean satellites to the Jovian magnetosphere. Geophys. Res. Lett., 5, 155-158.

Larson, H.A., Fink, U. & Treffers, R.R. (1978) Evidence for CO in Jupiter's atmosphere from airborne spectroscopic observations at 5 microns. Astrophys. J., 219, 1084-1092.

Larson, H.P., Fink, U., Treffers, R.R. & Gautier, T.N. (1975) Detection of water vapor on Jupiter. Astrophys. J., 197, L137-L140.

Larson, H.P., Treffers, R.R. & Fink, U. (1977) Jupiter's atmosphere: the evidence from high-altitude observations at 5 micrometers. Astrophys. J., 211, 972-979.

Lewis, J.S. (1969) The clouds of Jupiter and the NH_3-H_2O and NH_3-H_2S systems. Icarus, 10, 365-378.

Lewis, J.S. (1980) Lightning synthesis of organic compounds on Jupiter. Icarus, 43, 85-95.

Lewis, J.S. & Prinn, R.G. (1970) Jupiter's clouds: structure and composition. Science, 169 472-473.

Leyko, J. (1964) Equilibrium studies on the H_2S-NH_3-H_2O system. I. Bull. Acad. Polon. Sci. Ser. Chim., 12, 275.

Linke, W.F. (1965) Solubilites of Inorganic and Metalorganic Compounds. Fourth Edition, Washington D.C.: American Chemical Society.

Lowenstein, R., Harper, D. & Moseley, H. (1977) The effective temperature of Neptune. Astrophys. J. Lett., 218, 145.

Mason, B.J. (1957) The Physics of Clouds. New York: Oxford University Press.

Massie, S.T. & Hunten, D.M. (1982) Conversion of para and ortho hydrogen in the Jovian planets. Icarus, 49, 213-216.

McConnell, J.C., Holberg, J.B., Smith, G.R., Sandel, B.R., Shemansky, D. & Broadfoot, A.L. (1082) A new look at the ionosphere of Saturn in light of the UVS occultation results. Planet. Space Sci., 30, 151-167.

Morabito, J., Synott, S.P., Kupferman, P.N. & Collins, S.A. (1979) Discovery of currently article extraterrestrial volcanism. Science, 204, 972.

Mount, G.H., Warden, E.S. & Moos, H.W. (1977) Photoabsorption cross sections of methane from 1400-1850A. Astrophys. J., 214, L47-L49.

Palluconi, F.D. (1972) Atmospheric models. In The Planets Uranus, Neptune, and Pluto. NASA SP-8103.

Prather, M.J., Logan, J.A. & McElroy, M.B. (1978) Carbon monoxide in Jupiter's upper atmosphere: an extraplanetary source. Astrophys. J., 223, 1072-1081.

Prinn, R.G. & Barshay, S.S. (1977) Carbon monoxide on Jupiter and implications for atmospheric convection. Science, 198, 1031-1034.

Prinn, R.G. & Lewis, J.S. (1973) Uranus atmosphere: structure and composition. Astrophys. J., 179, 333-342.

Prinn, R.G. & Lewis, J.S. (1975) Phosphine on Jupiter and implications for the Great Red Spot. Science, 190, 274-276.

Prinn, R.G. & Olaguer, E.P. (1981) Nitrogen on Jupiter: a deep atmospheric source. J. Geophys. Res., to be published.

Prinn, R.G. & Owen, T.C. (1976) Chemistry and spectroscopy of the Jovian atmosphere. In Jupiter, ed. T. Gehrels, pp 319-371. Tucson: University of Arizona Press.

Ridgway, S.T., Wallace, L. & Smith, G.R. (1976) The 800-1200 inverse centimeter absorption spectrum of Jupiter. Astrophys., 207, 1002-1006.

Rottman, G. (1981) Rocket measurements of the solar spectral irradiance during solar minimum, 1972-1977. J. Geophys. Res., 86, 6697.

Sandel, B.R., Shemansky, D.E., Broadfoot, A.L., Holberg, J.B., Smith, G.R., McConnell, J.C., Strobel D.F., Atreya, S.K., Donahue, T.M., Moos, H.W., Hunten, D.M., Pomphrey, R.B. & Linick, S. (1982) Extreme ultraviolet observations from Voyager 2 encounter with Saturn. Science, 215, 548-553.

Science, (1979) Mission to Jupiter and its Satellites, 204, 945-1008.

Slanger, T.G. (1982) 1216A photodissociation of H_2O, NH_{23}, and CH_4. In Abstracts, Fourth Annual Meeting of Planetary Atmospheres Principal Investigators. April 21-23, 1982,

Ann Arbor, Michigan.
Strobel, D.F. (1969) The photochemistry of methane in the Jovian atmosphere. J. Atmos. Sci., 26, 909-911.
Strobel, D.F. (1973a) The photochemistry of NH_3 in the Jovian atmosphere. J. Atmos. Sci., 30, 1205-1209.
Strobel, D.F. (1973b) The photochemistry of hydrocarbons in the Jovian atmosphere. J. Atmos. Sci., 30, 489-498.
Strobel, D.F. (1975) Aeronomy of the major planets. Photochemistry of ammonia and hydrocarbons. Rev. Geophys. Space Phys., 13, 372-382.
Strobel, D.F. (1977) NH_3 and PH_3 photochemistry in the Jovian atmosphere. Astrophys. J. Lett., 214, 97-99.
Strobel, D.F. & Yung, Y.L. (1979) Production and accumulation of CO in the Jovian upper atmosphere. Icarus, 37, 256-263.
Teifel, V.G. (1983) Methane abundance in the atmosphere of Uranus. Icarus, 53, 389-398.
Tokunaga, A.T., Beck, S.C., Geballe, T.R., Lacy, J.H. & Serabyn, E. (1981) The detection of HCN on Jupiter. Icarus, 48, 283-289.
Tokunaga, A.T., Orton, G.S., Caldwell, J. (1983) New observational constraints on the temperature inversions of Uranus and Neptune. Icarus, 530, 141-146.
Tyler, G.L., Eshleman, V.R., Anderson, J.D., Levy, G.S., Lindal, G.F., Wood, G.E. & Croft, T.A. (1981) Radio science investigation of the Saturn system with Voyager 1: preliminary results. Science, 212, 201-206.
Vera Ruiz, H.G. & Rowland, F.S. (1978) Red phosphorus as the main chromophore in the Great Red Spot of Jupiter? Preprint.
Waite, J.H., Jr., Atreya, S.K. & Cravens, T.E. (1983) Effect of atomic hydrogen and vibrationally excited molecular hydrogen on the ionosphere of Saturn. In preparation.
Wallce, L. (1980) The structure of the Uranus atmosphere. Icarus, 43, 231-259.
Weidenschilling, S.J. & Lewis, J.S. (1973) Atmospheric and cloud structures of the Jovian planets. Icarus, 20, 465-476.
Wilson, J.A. (1925) The total and partial vapor pressures of aqueous ammonia solutions, U. III. Eng. Exp. Sta. Bull., 146.
Woeller, F. & Ponnamperuma, C. (1969) Organic synthesis in a simulated Jovian atmosphere. Icarus, 10, 386-392.